Study of the PAH Formation in Premixed Rich Flames of $C_6H_6/O_2/Ar$ and $C_6H_6/C_2H_2/O_2/Ar$

V. Detilleux, V. Dias and J. Vandooren

Laboratoire de Physico-Chimie de la Combustion
Université catholique de Louvain
Place Louis Pasteur, n°1
1348 Louvain-la-Neuve
Belgium

UCL Université catholique de Louvain BELGIUM

Aim of this work

- **Influence of acetylene on PAH concentration in rich $C_6H_6/O_2/Ar$ flame**

- **Comparison between experiment and simulation**

Formation of PAH

Three hypothesis

From *cyclopentadienyl* (*The C_5 way*)

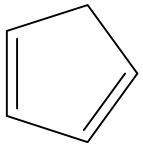

Marinov and al., 1997

The HACA mechanism (*H Abstraction – C_2H_2 Addition*)

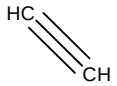

Frenklach and al., 1984

Initiation by *Benzene – Phenyl addition*

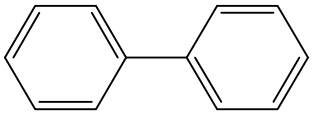

Frenklach and al., 1986

UCL Université catholique de Louvain BELGIUM

Experimental Flames

Comparison of two flames

$\phi = 2.0$ P = 45 mbar

FB $C_6H_6/O_2/Ar$

11.5% C_6H_6

43.2% O_2

45.3% Ar

$C_6H_6/C_2H_2/O_2/Ar$ **FBA**

10.7% C_6H_6

2.6% C_2H_2

43.2% O_2

43.5% Ar

Comparison of mole fraction for intermediate species and PAH

Experimental Setup

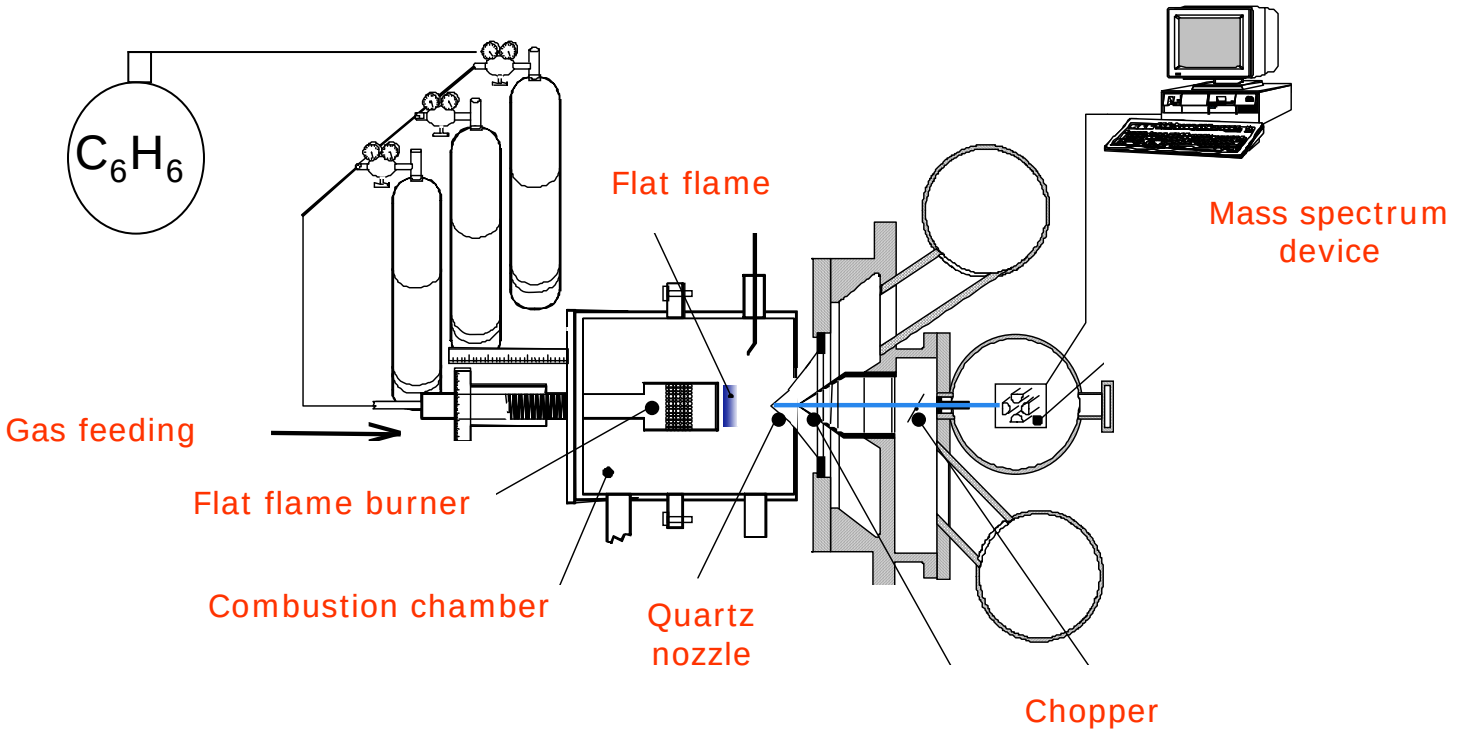

Flat flame burner
45 mbar

UCL Université catholique de Louvain BELGIUM

Main Chemical Species

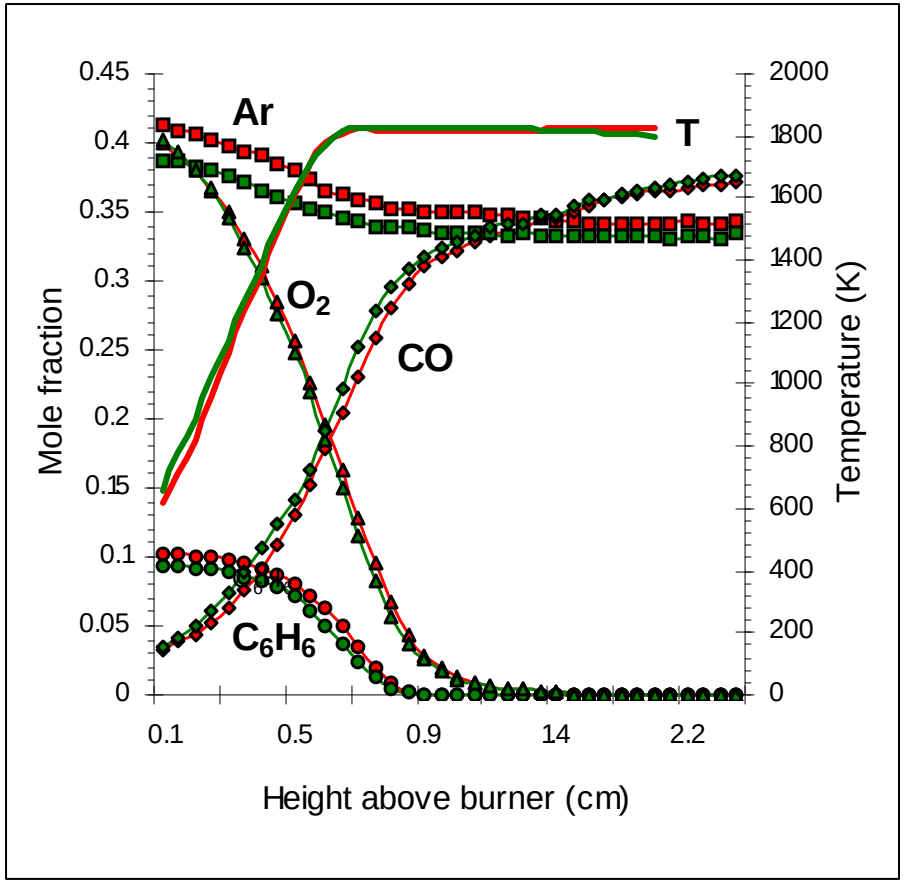

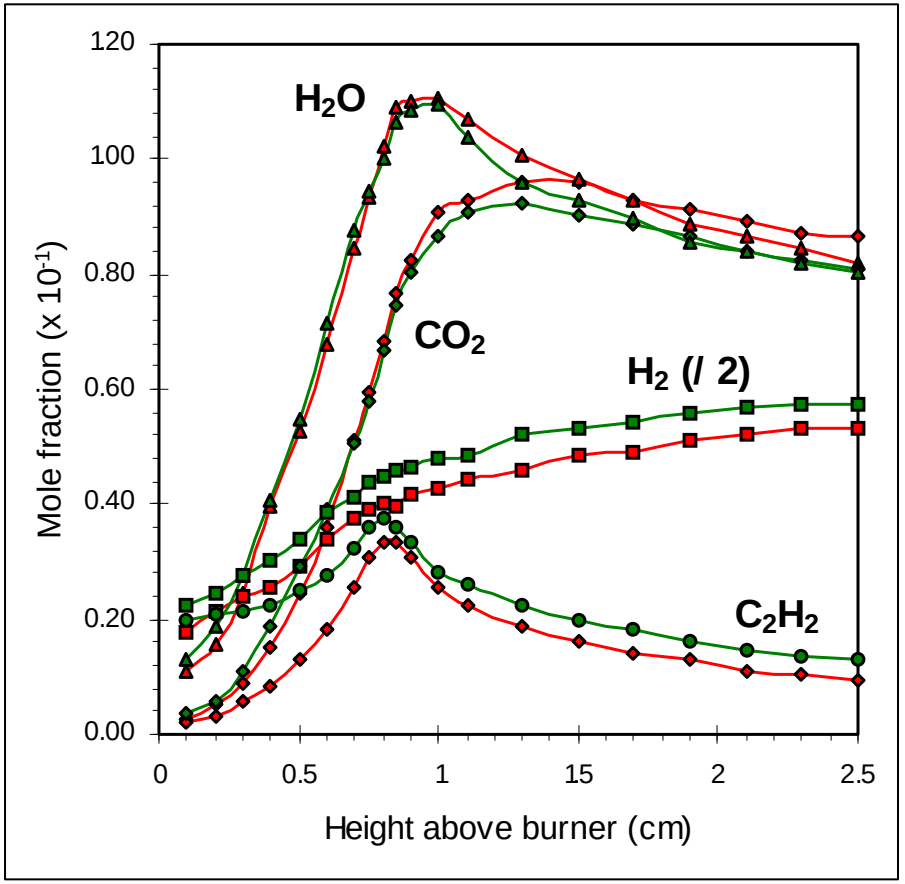

FB

FBA

UCL Université catholique de Louvain BELGIUM

Intermediate Chemical Species

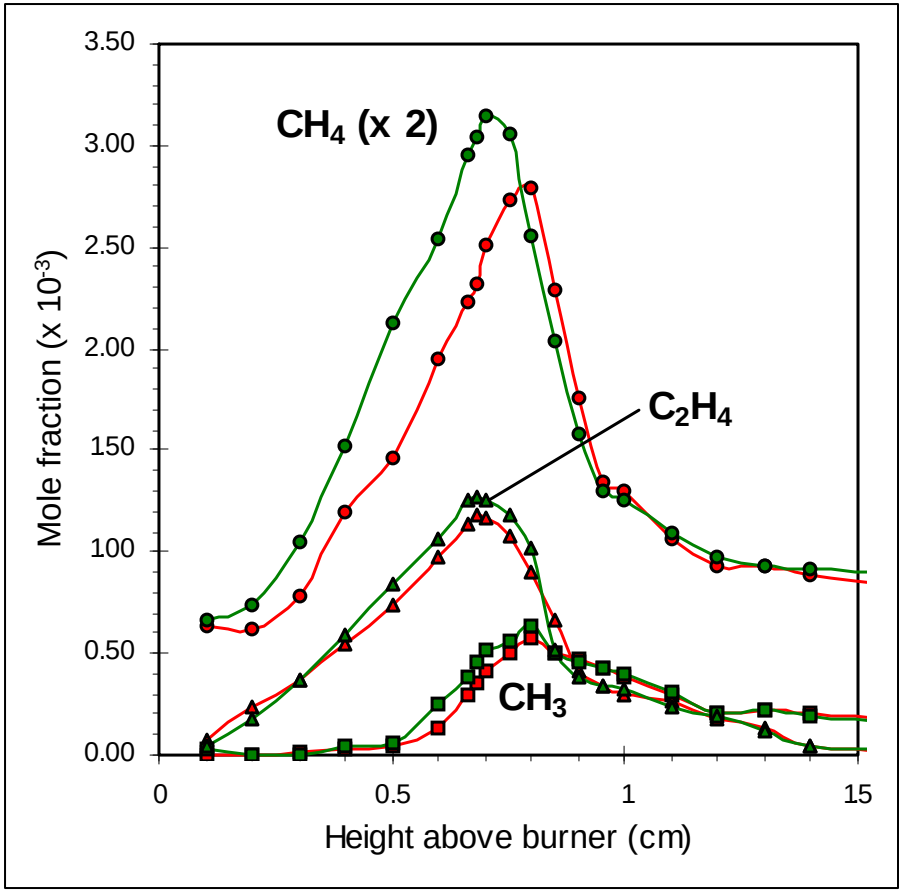

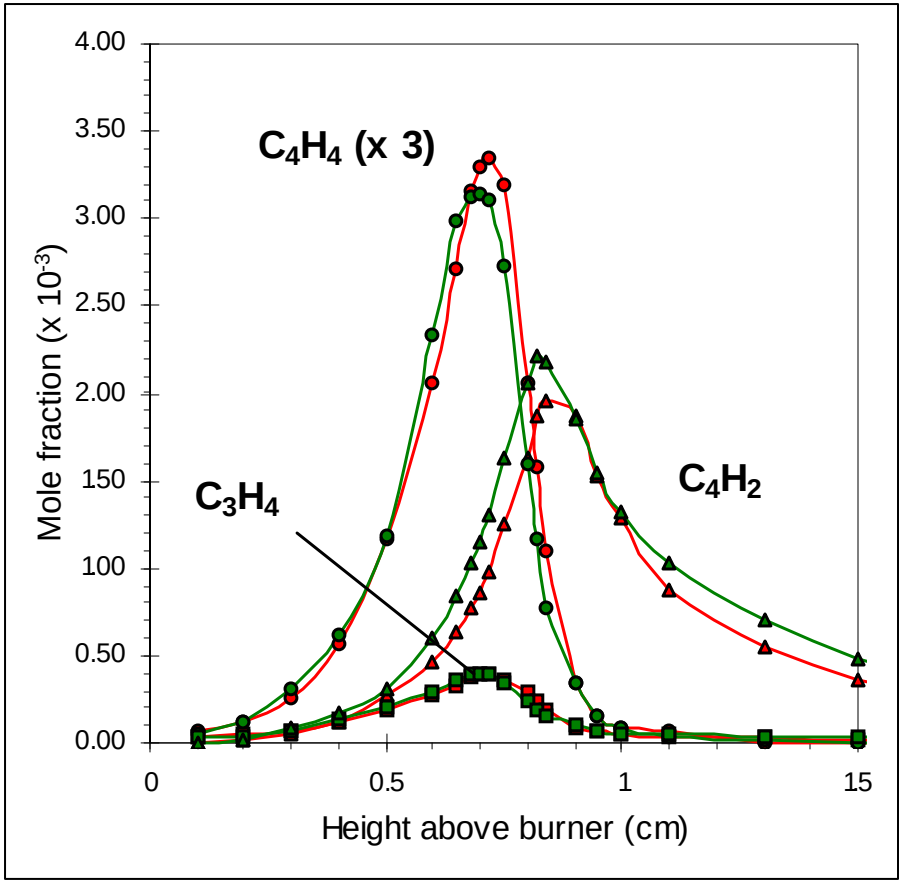

FB

FBA

UCL Université catholique de Louvain BELGIUM

Intermediate Chemical Species

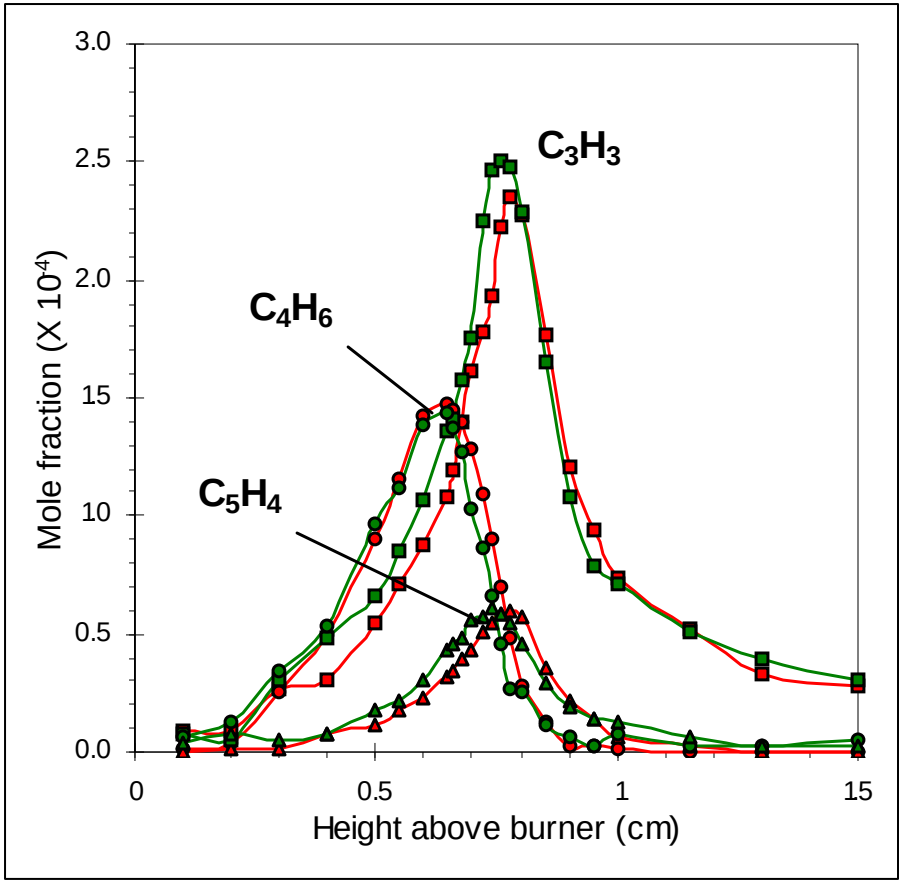

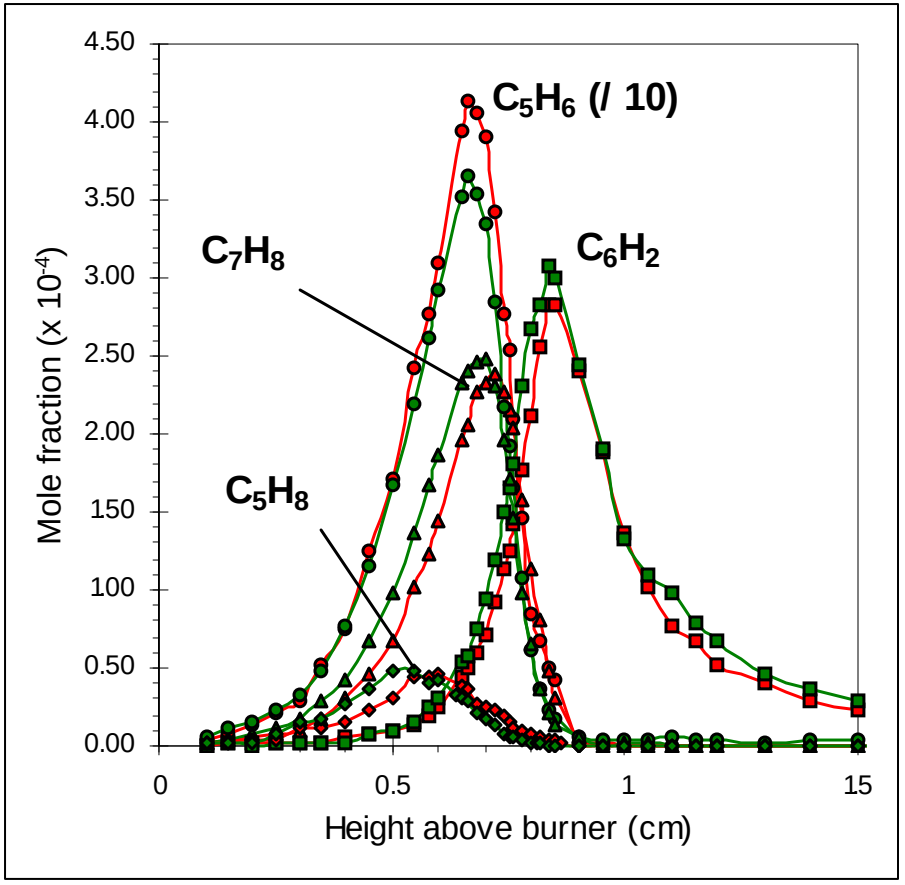

FB

FBA

UCL Université catholique de Louvain BELGIUM

Intermediate Chemical Species

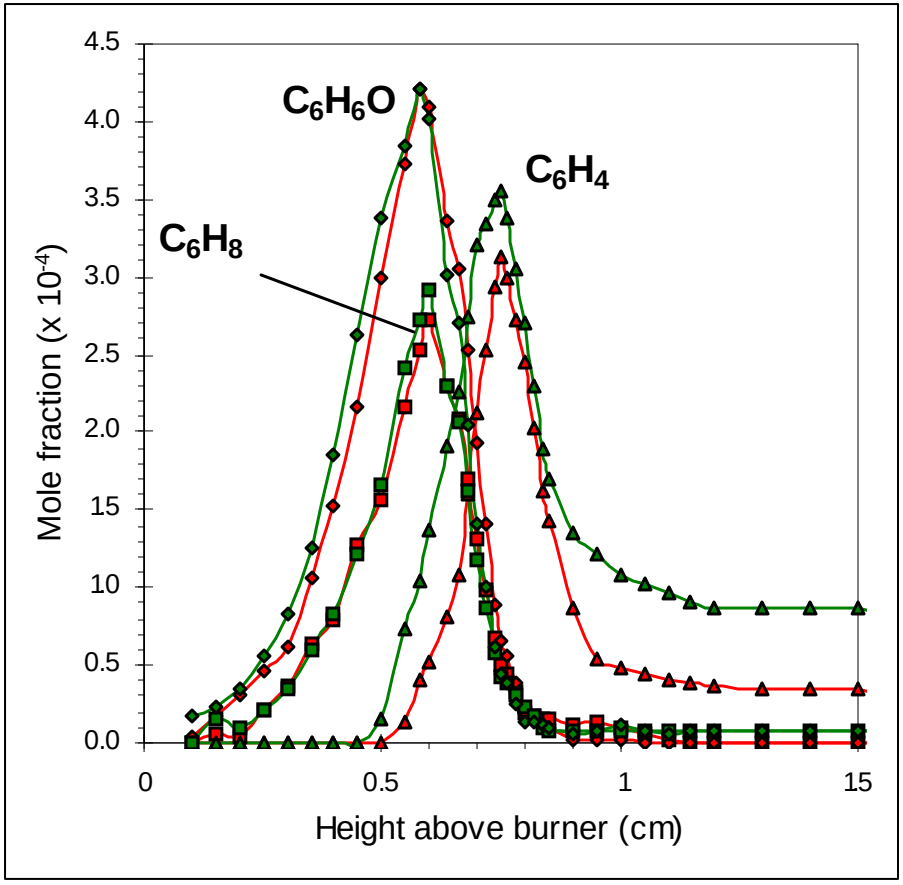

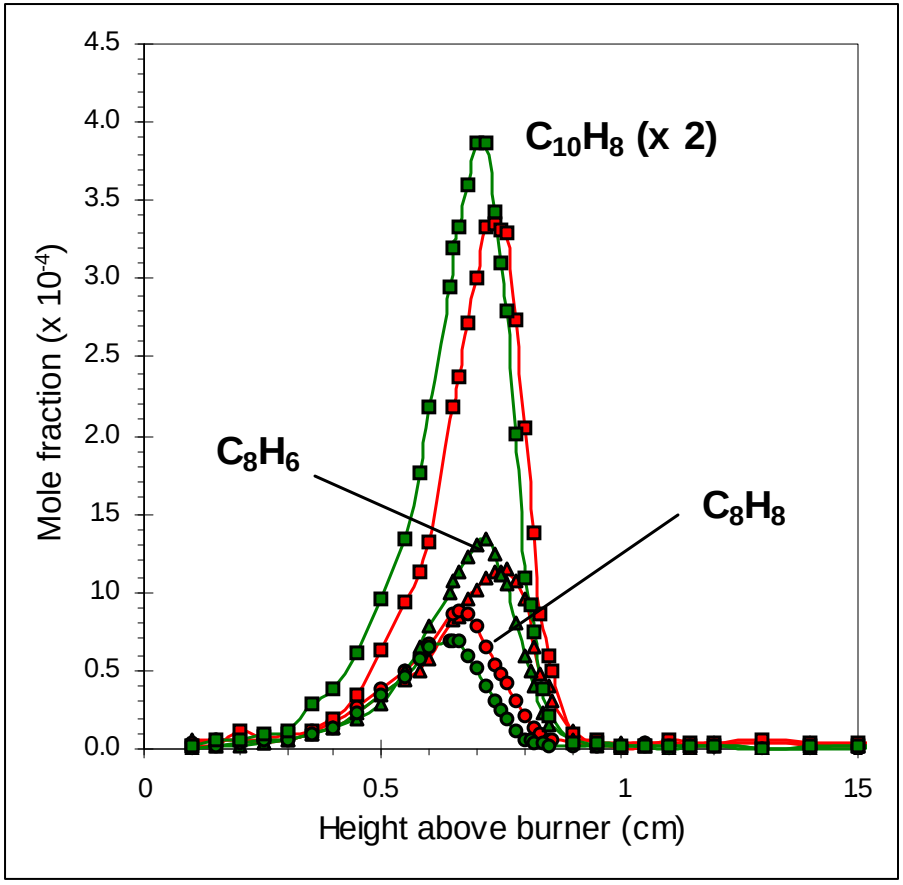

FB

FBA

UCL Université catholique de Louvain BELGIUM

Intermediate Chemical Species

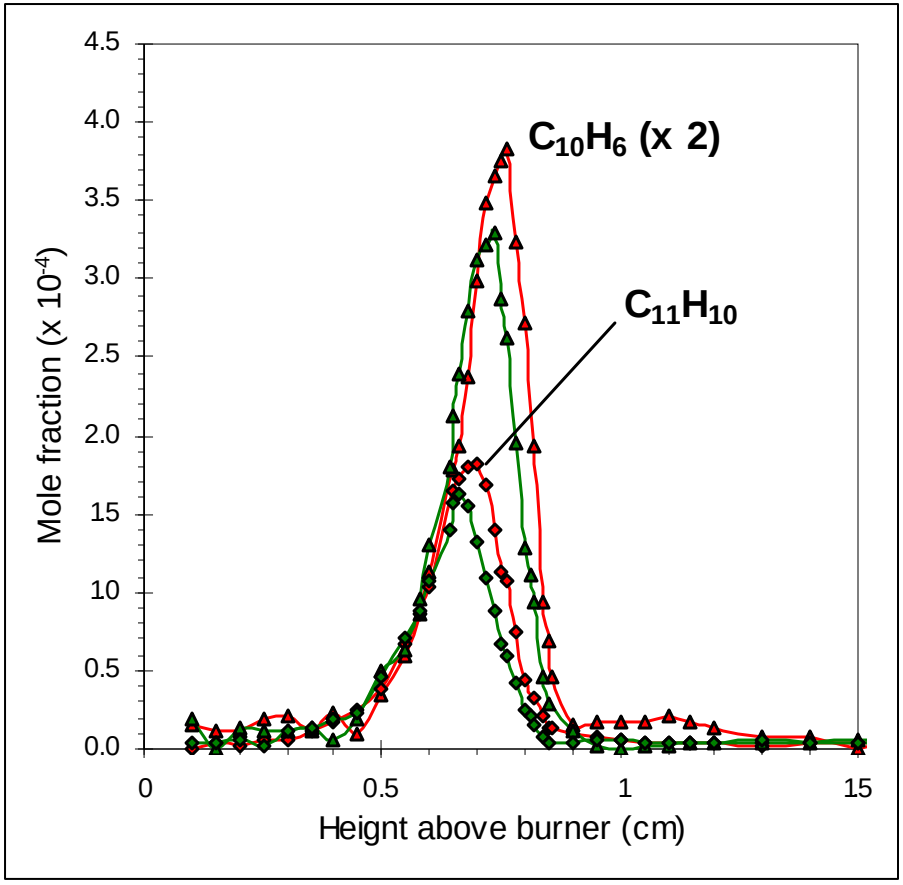

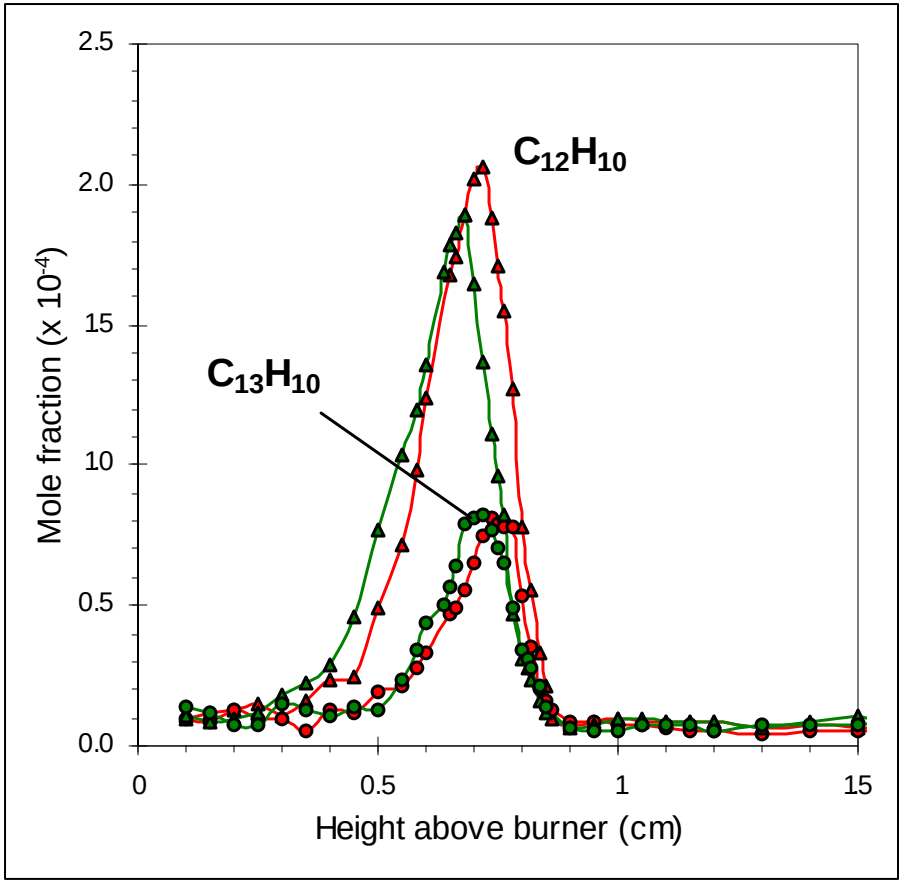

FB

FBA

Intermediate Chemical Species

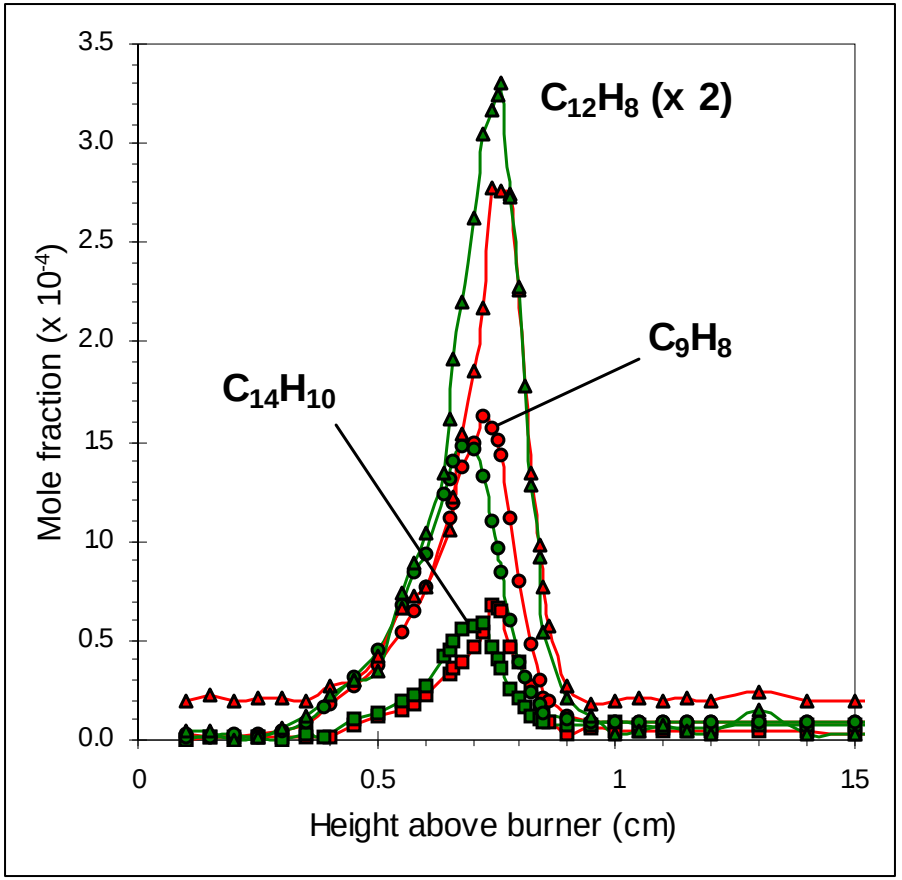

FB

FBA

UCL Université catholique de Louvain BELGIUM

Phenanthrene Formation Pathways

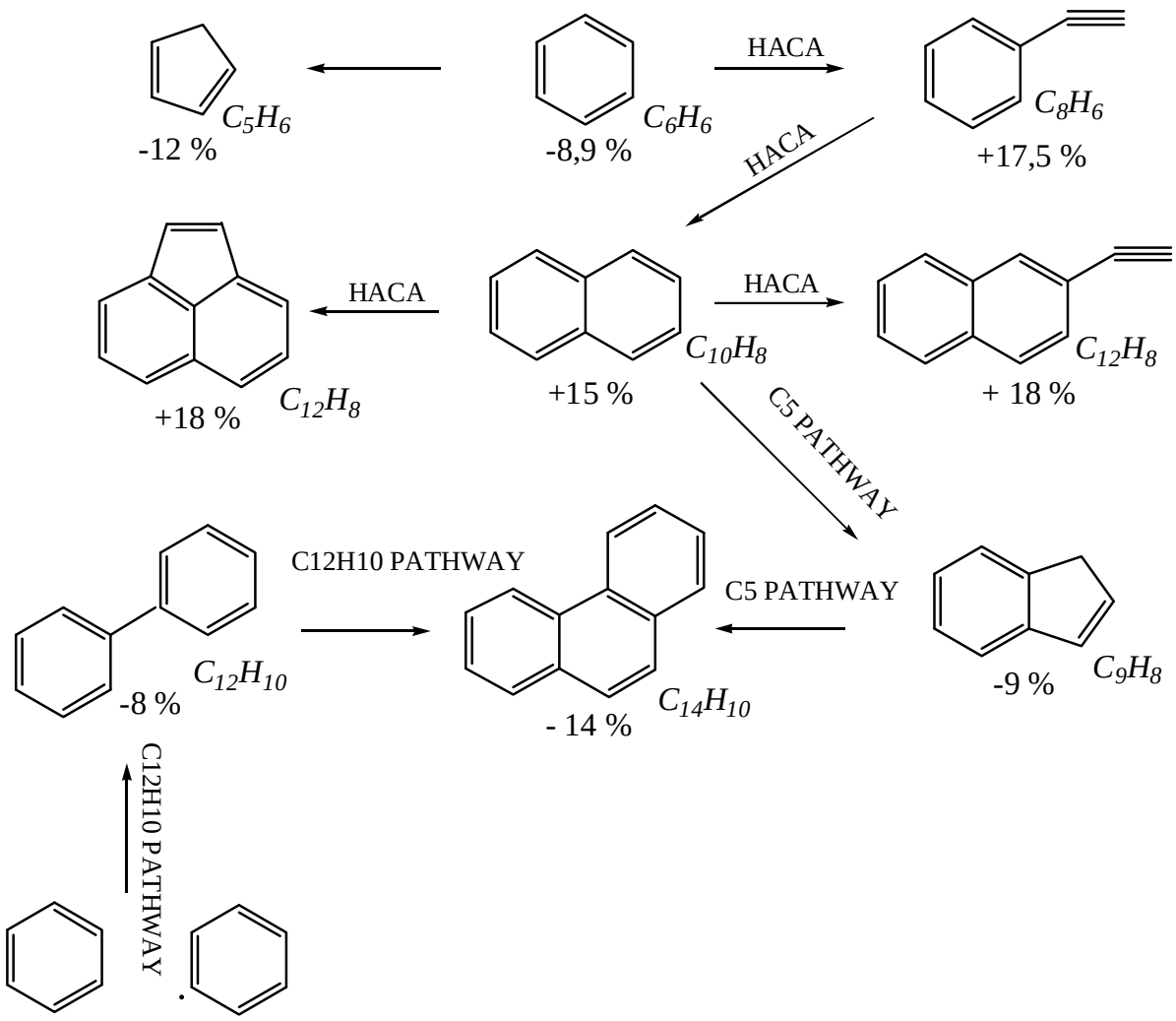

UCL Université catholique de Louvain BELGIUM

Experimental Conclusions

1. General observations:

- FBA produces less CO_2 and more H_2 than FB
- The degradation of C_6H_6 into acetylene is faster than C_2H_2 consumption

2. About PAH formation:

- $C_{10}H_8$ seems to be produced by the HACA mechanism
- $C_{14}H_{10}$ does not seem to be formed by the HACA mechanism
  → C_5 Pathway ?
- The mole fractions of other PAH increase when using C_2H_2 as co-reactant

UCL Université catholique de Louvain BELGIUM

Kinetic Model

- ***Original reaction mechanism (Dias, 2003)*:**
  402 reactions – 78 chemical species (C_1 to C_{10})

  Validated against premixed rich $C_2H_6/O_2/Ar$, $C_2H_4/O_2/Ar$, $C_2H_2/O_2/Ar$ and $CH_4/O_2/Ar$ flames by *Dias et al. (2003)*

- **Simulation of the kinetic mechanism by using of COSILAB and the measured temperature profiles of FB and FBA**

- **Validation of the new mechanism by comparing simulated mole fraction profiles with MBMS experimental results**

Dias, V. (2003) PhD Thesis Université catholique de Louvain, Belgium

Dias V., Van Tiggelen, P.J. and Vandooren, J. (2003) Proc. of European Combustion Meeting, p.221

UCL Université catholique de Louvain BELGIUM

Mole Fraction Profiles (Experimental and Simulated)

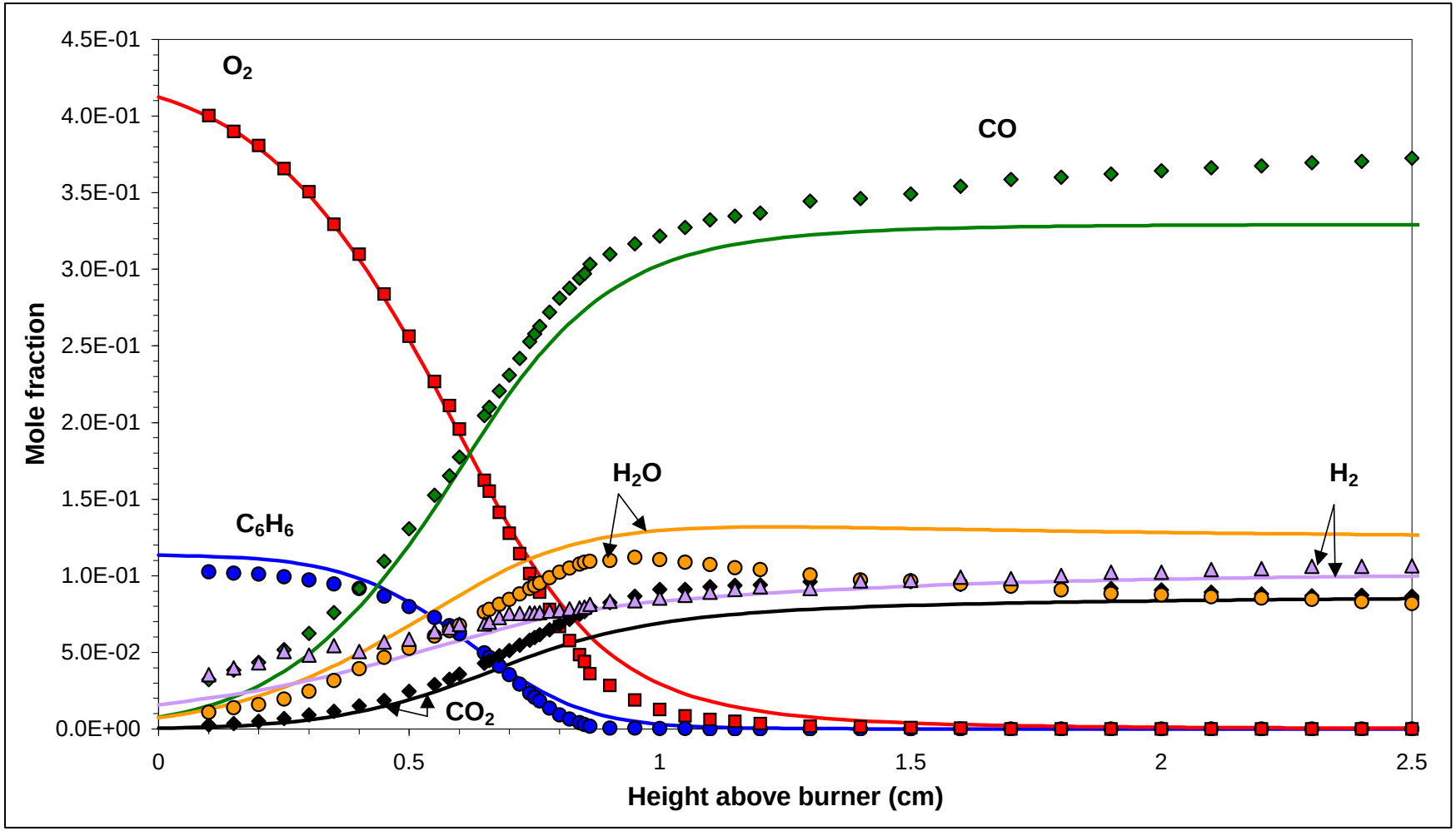

UCL Université catholique de Louvain BELGIUM

Mole Fraction Profiles (Experimental and Simulated)

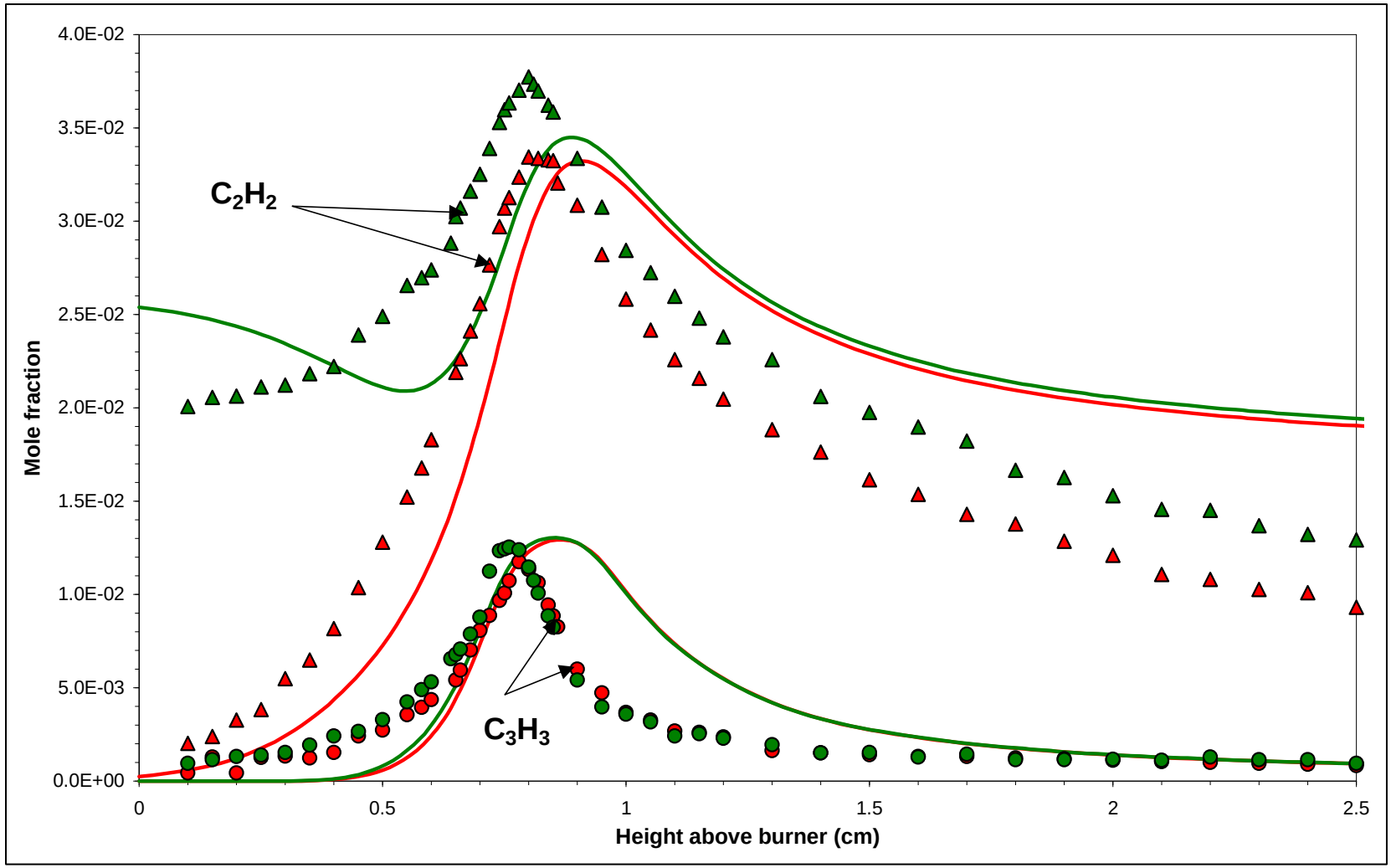

FB

FBA

UCL Université catholique de Louvain BELGIUM

Mole Fraction Profiles (Experimental and Simulated)

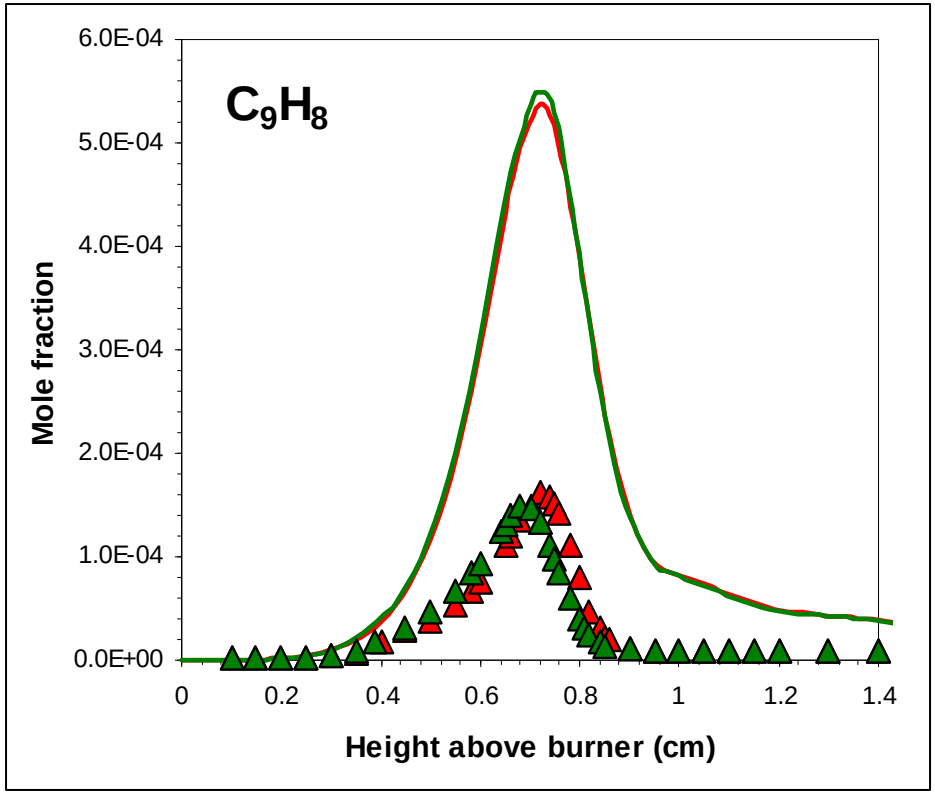

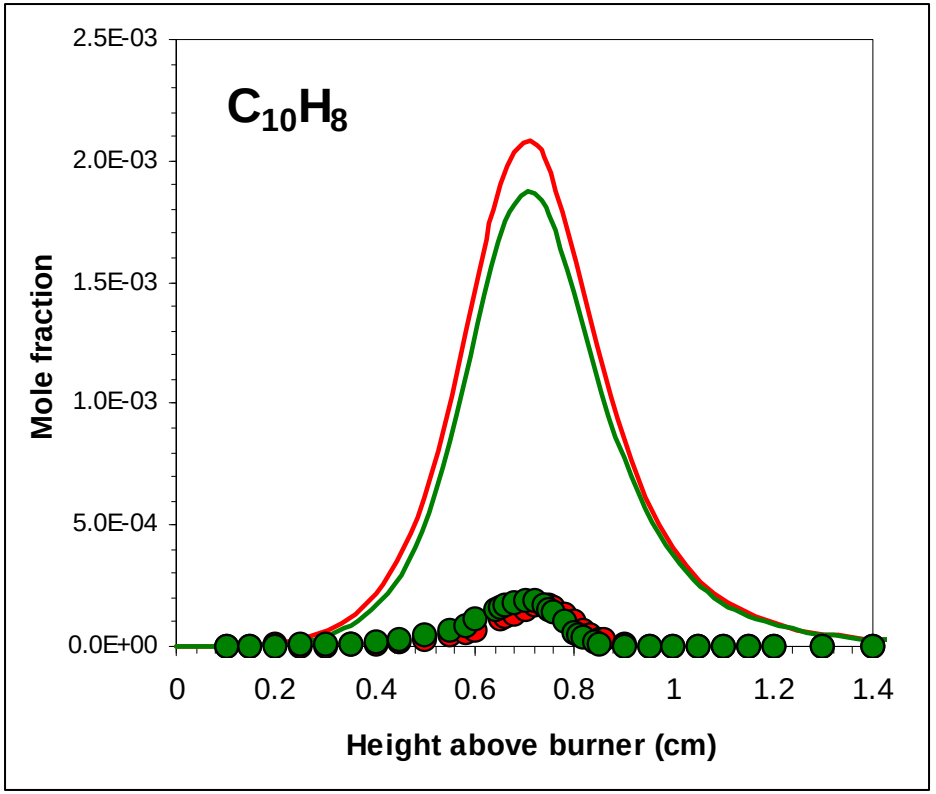

FB

FBA

UCL Université catholique de Louvain BELGIUM

Conclusions about Simulation

- ***For main species:*** **excellent agreement between experimental and simulated results.**

- ***For acetylene:*** **the kinetic model underestimates the reaction rate of production of C_2H_2 from the benzene, or overestimates the reaction rate of consumption of C_2H_2 in the flame front.**

- ***For heavier species than benzene:*** **the simulation overestimates in an important way the experimental mole fraction values. The mechanism is not taking into account reaction pathways for compounds heavier than naphthalene, therefore, it can not predict the consumptions of the species with more than six carbons.**

UCL Université catholique de Louvain BELGIUM

General Conclusions and Perspectives

1. General Conclusions:

- Acetylene seems to have an important impact on the PAH formation in $C_6H_6/O_2/Ar$ flames.
- Phenanthrene is not formed using the HACA pathway?
- A certain kinetic error for some species emerges from the Dias mechanism (ex: formation of $C_{10}H_8$, by the way of C_5 or by the HACA pathway??).

2. Perspectives:

- This MBMS analysis should be completed by a GC investigation in order to separate mass isomers and study heavier PAH.
- The Dias mechanism should be improved for some species and then, be completed to model all the present species in FB and FBA (until $C_{18}H_{10}$).

UCL Université catholique de Louvain BELGIUM

Acknowledgements

The authors are very grateful to the Ministère de la Région Wallonne (Belgium) for the financial support.

o **The C_5 Way :**

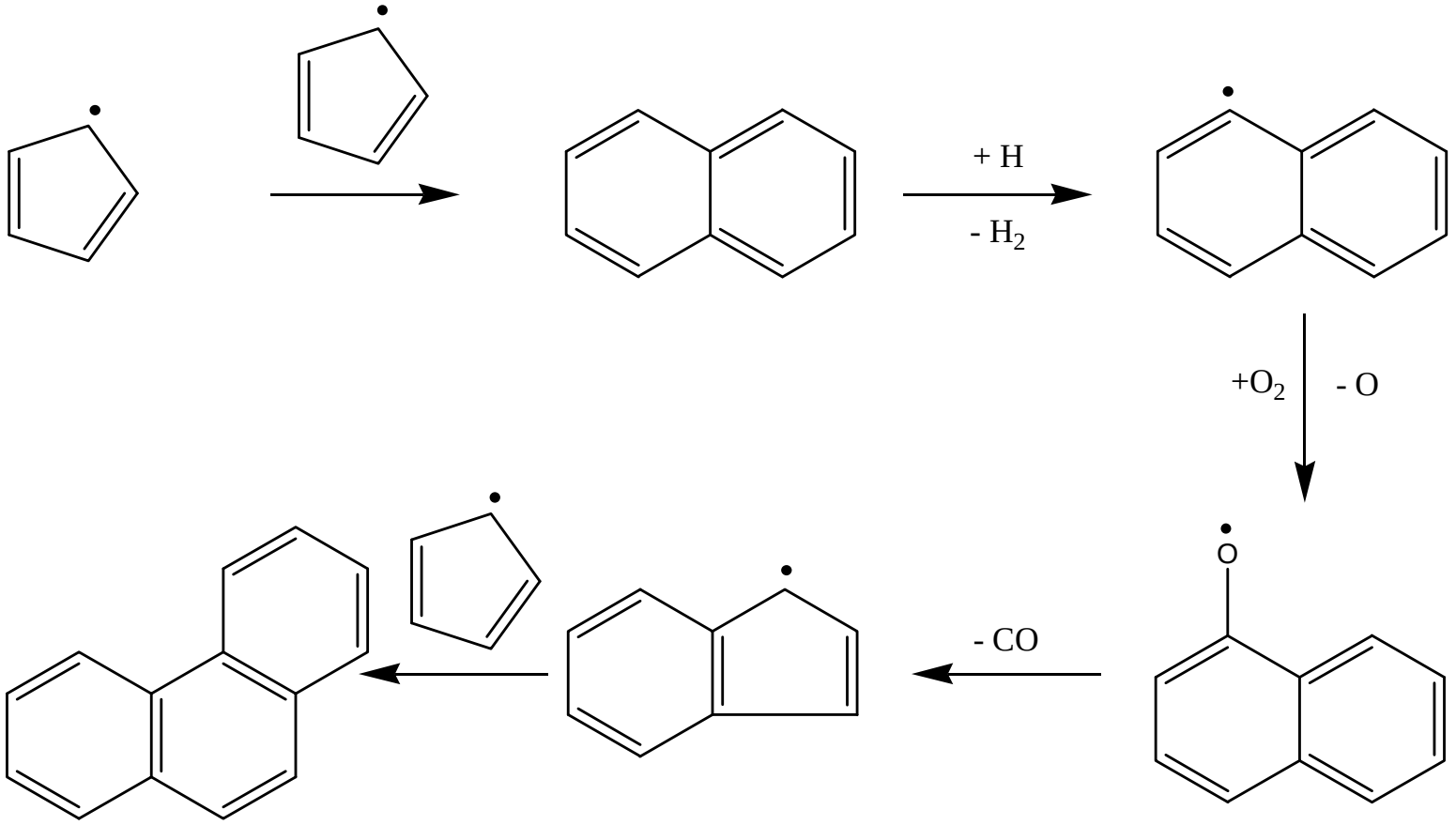

o The HACA mechanism

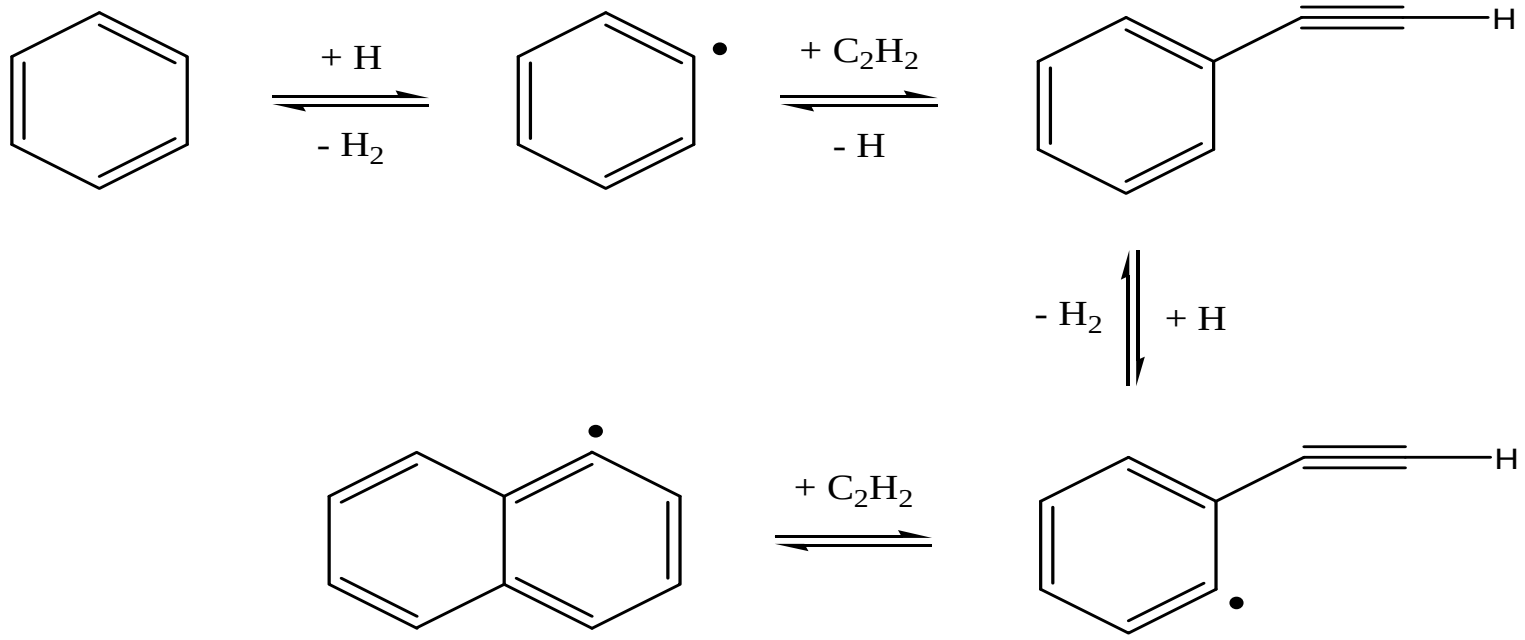

Hypothesis :

If the concentration of C_2H_2 in the flame increases, the production of PAH will go up

o Initiation by benzene – phenyl addition

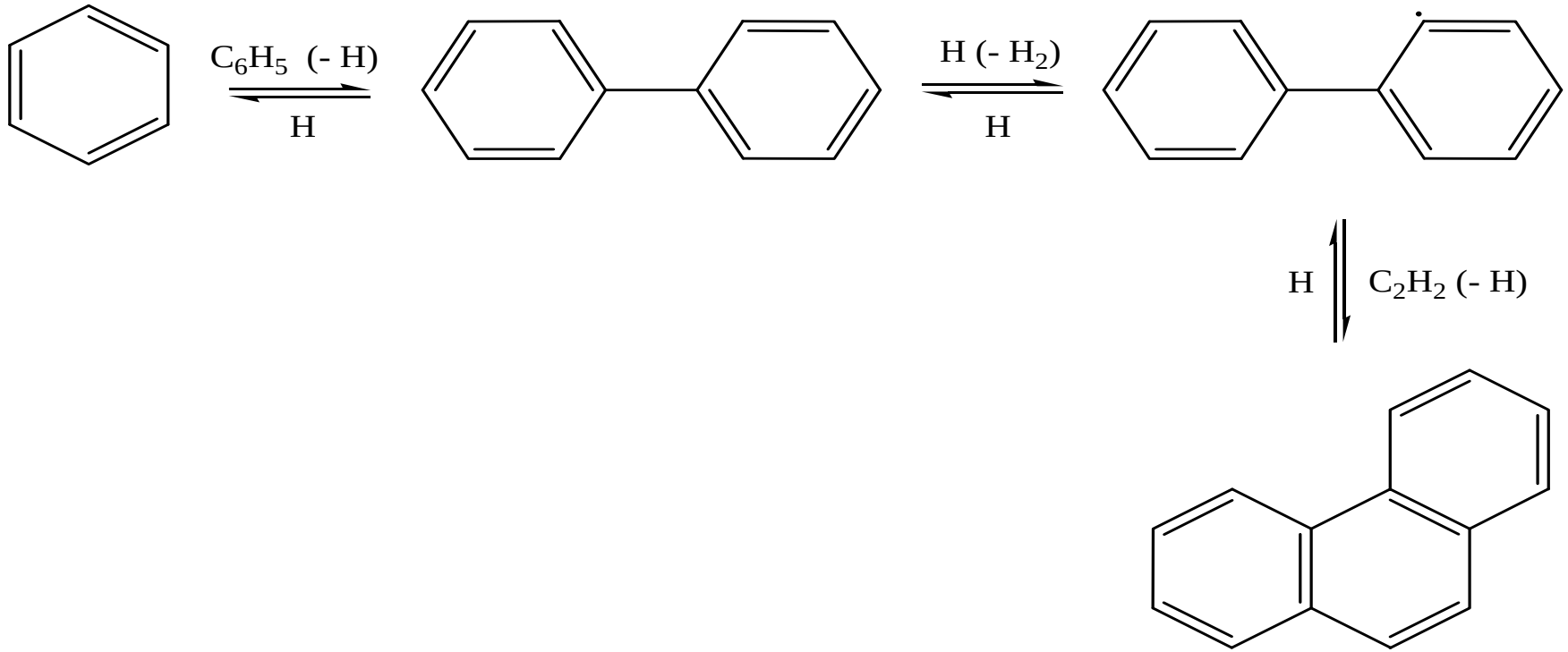

Subtask 2.4F

Study of the PAH Formation in Premixed Rich Flames of $C_6H_6/O_2/Ar$ and $C_6H_6/C_2H_2/O_2/Ar$

Valéry Detilleux, Véronique Dias and Jacques Vandooren
CSTR – Laboratoire de Physico-Chimie de la Combustion
Université catholique de Louvain
Place Louis Pasteur, 1 - 1348 Louvain-la-Neuve - Belgium

ABSTRACT

The combustion of hydrocarbons in rich flames leads to the formation of PAH (Polycyclic Aromatic Hydrocarbons). Many PAH are known to be carcinogenic and play an important role in the process of soot formation. Thus it is essential to investigate the pathways by which they are formed, in order to inhibit their production.
Nowadays, three main sources of PAH production are suggested: the cyclopentadienyl pathway (Marinov et al., 1996 ; Castaldi et al. 1996), the HACA mechanism (Frenklach and Wang, 1990), and the biphenyl pathway (Frenklach et al., 1986).

The aim of this work is to measure the structure of rich premixed flames of benzene-oxygen-argon (11.5 % C_6H_6 - 43.2 % O_2 - 45.3 % Ar) and benzene-acetylene-oxygen-argon (10.7 % C_6H_6 - 2.6 % C_2H_2 - 43.2 % O_2 - 43.5 % Ar), both with an identical equivalence ratio of two, stabilised at low pressure (45 mbar). Identification and monitoring of chemical species were performed by molecular beam mass spectrometry (MBMS). Since benzene is an important precursor of PAH and acetylene is supposed to be an essential intermediate in their formation, the analysis and comparison of these flame structures will allow us to evaluate more precisely the role of C_2H_2 in PAH production.
By using the DIAS (Dias, 2003 ; Dias et al., 2003) mechanism, numerical simulations have been carried out to predict mole fraction profiles, until naphthalene.
The whole comparison, between the two flames and with simulated data, will provide important clues about the role of C_2H_2 in reactions leading to the formation of PAH.

Introduction

For some years, human people awakes to the consciousness of environmental consequences of their industrial development. In the area of hydrocarbons combustion, the understanding of the formation of Polycyclic Aromatic Hydrocarbons (PAH) is one of the main goals, in order of their threat to the human health (Dockery et al., 1993 ; Siegmann and Siegmann, 1998).

An attractive way to investigate PAH formation pathways is the analysis of laminar and low pressure rich benzene flame structures, where the first aromatic ring (benzene) does not have to be formed. In these conditions, Bittner and Howard, in their pioneer works of 1981, observed numerous PAH and suggested a two-steps acetylene addition to explain their formation (Bittner and Howard, 1981).

According to numerical investigations, realised by Frenklach and Wang (1990), this two-steps pathway – named the HACA pathway for H-Abstraction-C_2H_2-Addition – is a dominant route to larger PAH formation (Frenklach et al., 1984 ; Frenklach and Warnatz, 1987).
Moreover, Frenklach and al. (1986) identified the addition of benzene to phenyl radical (C_6H_5), resulting in biphenyl ($C_{12}H_{10}$), as another principal pathway leading to PAH formation. In this route, the biphenyl production is followed by a sequential addition of two acetylene molecules to form pyrene ($C_{16}H_{10}$). Afterwards, this four peri-condensed PAH can growth following the HACA process.
In 1996, Marinov and al. (1996) have performed experimental and kinetic modelling studies of PAH formation in methane and ethylene rich flames (Castaldi et al. 1996). In order to explain the PAH levels observed, they proposed a new pathway to produce larger aromatic chemical species in which two cyclopentadienyl radicals (C_5H_5) combine and rearrange to form naphthalene ($C_{10}H_8$).

Many authors have developed kinetic models in order to simulate numerically experimental data on hydrocarbons and PAH evolution measured in flames (Marinov et al., 1998 ; Wang and Frenklach, 1997 ; Richter et al., 1999 ; Rasmussen et al., 2005). At the present time, no one succeeds in building up a global kinetic model, with a proper consensus of the different pathways presented above, able to describe correctly all experimental observations. Previously, Dias (2003) has developed a reaction mechanism validated against premixed rich $C_2H_4/O_2/Ar$ flames (ϕ = 2.25 and 2.50) which describes in detail the formation of soot precursors, until the naphthalene. This mechanism could be extent to the larger PAH to model these benzene flames.

The aim of this work is, firstly, to analyse the structure of rich premixed $C_6H_6/O_2/Ar$ and $C_6H_6/C_2H_2/O_2/Ar$ flames, both with an identical equivalence ratio of two. Since benzene is an important precursor of PAHs and acetylene is supposed to be an essential intermediate in their formation, the analysis and comparison of these flame structures have allowed us to evaluate more precisely the role of C_2H_2 in hydrocarbons and PAH production.
The second part of this work is to test the mechanism elaborated by Dias (2003) in these two rich benzene flames to model species until the naphthalene, before to extent it for the formation of larger PAHs (until $C_{18}H_{10}$).

Experimental Setup

The experimental setup used to carry out the analysis was well described previously by Vandooren et al. (1992) and Dias et al. (2004). Briefly, it consists in a combustion chamber where a flat flame is stabilized at low pressure (45 mbar) on a movable burner of 8 cm in diameter (Fig. 1). In front of the burner is a conical quartz nozzle with a 45° angle within 2 cm and with a small hole of 0.2 mm. This nozzle and the movable burner allow sampling to be performed at different heights of the flame. Behind the quartz cone, three differentially pumped chambers lead to the formation of a molecular beam that is directed to the electronic ionization source of a quadrupole mass spectrometer (EXTREL C50), as presented in Fig. 1. The formation of a molecular beam allows the initial sampling to be “frozen” until it reaches the analysis device ; thus, reactive chemical species as radicals are detected and monitored. Moreover, the molecular beam is chopped at 30 Hz for phase detection and monitoring, allowing the enhancement of the signal-to-noise ratio.

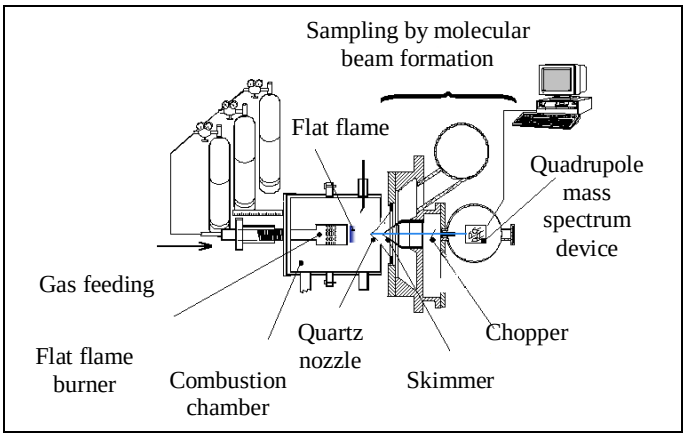

Figure 1: Experimental setup

The intensity signals have been recorded with an ionization potential carefully selected, depending on the chemical species under investigation, in order to maximize signal-to-noise ratio and avoid fragmentation interferences. Every chemical species were analysed simultaneously in both flame and in similar conditions in order to perform a reliable calibration and a direct comparison. An absolute calibration of chemical species present in the $C_6H_6/O_2/Ar$ flame (FB: reference flame), was performed by Defoeux et al. (2005). Calibration of the $C_6H_6/C_2H_2/O_2/Ar$ flame (FBA) have been performed by direct comparison with the reference flame through the equation :

$$[X_i]_{z,FBA} = \frac{[X_i]_{z,FB}}{[I_i]_{z,FB}} \cdot [I_i]_{z,FBA}$$

where I, X, i and z are the signal intensity, the mole fraction, the chemical species under investigation and the height above the burner, respectively.

Temperature measurements at different heights of the flame have been accomplished by using a Pt/PtRh10% thermocouple, 0.1 mm in diameter, coated with a thin layer of Y_2O_3-BeO ceramic to prevent catalytic effects of Pt on chemical reactions occurring in the flame. Data acquired have been corrected for radiation losses by the electrical compensation method.

Experimental Results and Discussion

One dimensional benzene-oxygen-argon (FB: 11.5 % C_6H_6 - 43.2 % O_2 - 45.3 % Ar) and benzene-acetylene-oxygen-argon (FBA: 10.7 % C_6H_6 - 2.6 % C_2H_2 - 43.2 % O_2 - 43.5 % Ar) flames, both with equivalence ratio of two, were stabilized at low pressure (45 mbar) on the flat flame burner. In the following figures, empty and full symbols represent FB and FBA, respectively.

Figs. 2 and 3 show temperature evolution and mole fraction profiles of main chemical species in FB and FBA (dashed line for FBA and continuous line for FB). Equivalence of both temperature profiles avoids temperature to be responsible of differences observed in flame structures. Therefore, a reliable and direct mole fraction comparison of both flames is allowed. As expected by fresh gases compositions, the mole fractions of C_6H_6 and Ar, next to the burner, are lower in FBA, whereas C_2H_2 mole fraction is higher. In both flames, according to the fall off of their mole fraction profile to zero, at 0.9 and 1.3 cm above the burner

respectively, reactants C_6H_6 and O_2 are completely consumed. In the burned gases only few compounds subsist in relatively high concentration: CO, CO_2, H_2O, H_2 and C_2H_2.
In FBA, no critical mole fraction change is observed except for H_2 and C_2H_2. The maximum acetylene mole fraction increases by 13 % in FBA. However, this increment is lower than the one measured next to the burner. Therefore, additional C_2H_2 is partially consumed in FBA even if mole fraction profile does not drop down before it reaches a high. This important observation reveals that acetylene formation through benzene decomposition or pyrolysis is much faster in this region. The presence of acetylene in fresh gases rises up the molecular hydrogen mole fraction all along the flame. At 2.5 cm above the burner, the increment reaches 8.6 % of the amount measured in FB. Since acetylene is a fundamental reactant of HACA pathway and H_2 an essential product, molecular hydrogen increase could be linked to HACA stimulation through reactions:

$$A_i + H = A_i\bullet + H_2 \qquad \text{(R. 1)}$$
$$A_i\bullet + C_2H_2 = \text{products} \qquad \text{(R. 2)}$$

where A_i is an aromatic molecule with i peri-condensed cycle and $A_i\bullet$ its radical (Frenklach, 2002), as testified by maximum mole fraction increase of HACA intermediate species, such as C_8H_6, $C_{10}H_8$ and $C_{12}H_8$.

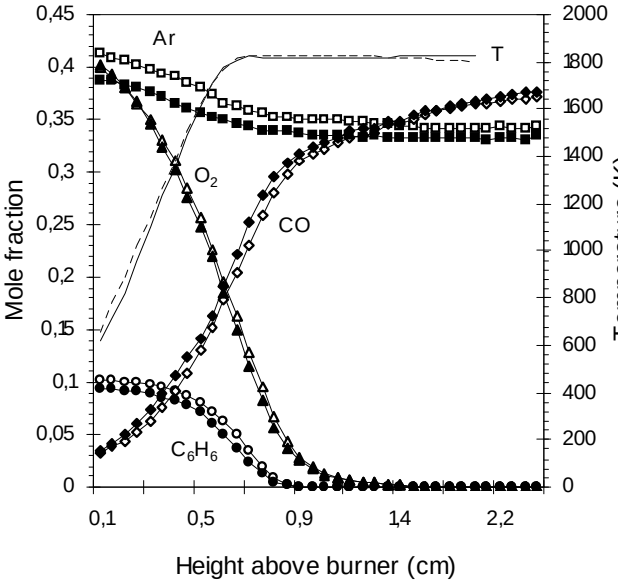

Figure 2 (symbols : empty = FB, full = FBA)

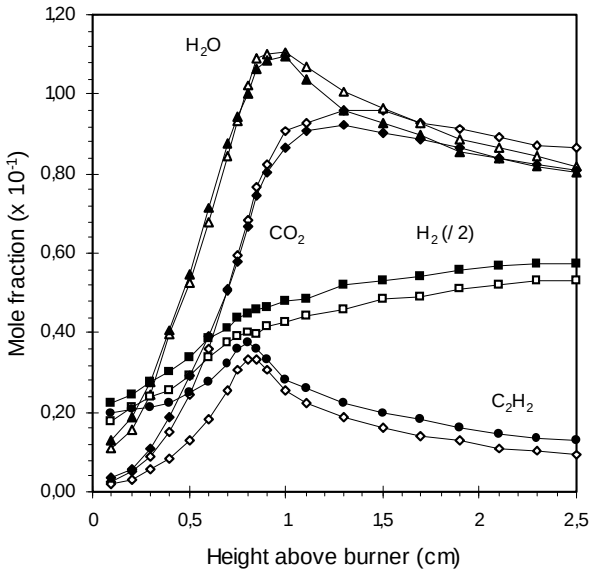

Figure 3 (symbols : empty = FB, full = FBA)

Fig. 4 presents mole fraction profiles of C_1 and C_2 hydrocarbons. Methyl radical and methane maximum mole fraction increase by 6 % and 13 % respectively in FBA. In this flame, acetylene, present as a reactant, provides C_1 and C_2 chemistry directly, rising up their concentration (Warnatz, 1984). The most important increase of methane mole fraction testifies that CH_3 is not the unique precursor of CH_4. Ethylene maximum mole fraction increases by 7 % in FBA.

Fig. 5 shows that no significant change is recorded on the maximum C_3H_4 mole fraction. However, the polyacetylenic C_4H_2 production is stimulated in FBA where its maximum mole

fraction increases by 12 %. The position and increment of mole fraction maximum are similar for acetylene, C_4H_2 and C_6H_2 polyacetylenic species. This observation testifies that $C_{2n}H_2$ compounds are mainly formed from C_2H_2 molecules. The maximum mole fraction of C_4H_4 decreases by 6 % in FBA, demonstrating the high dependence of C_4H_4 production pathways on benzene decomposition.

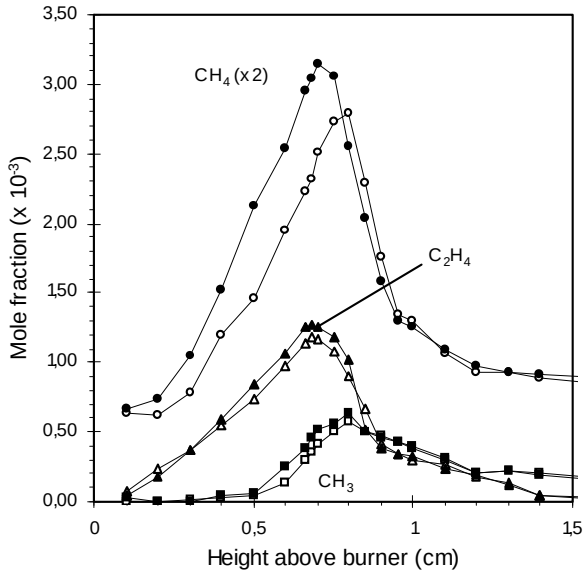

Figure 4 (symbols : empty = FB, full = FBA)

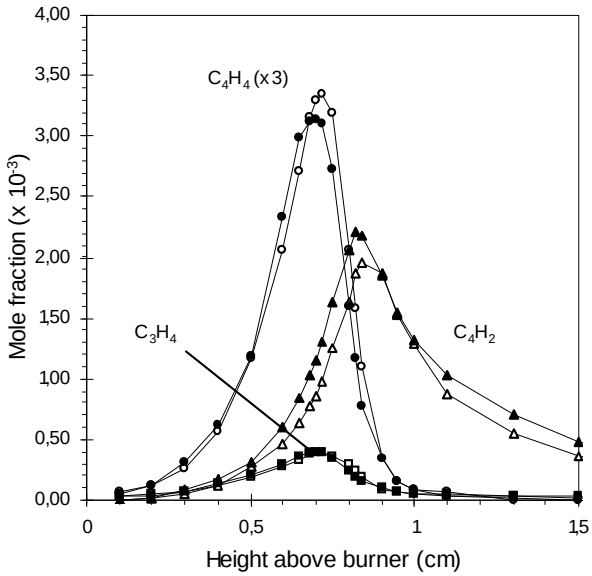

Figure 5 (symbols : empty = FB, full = FBA)

In Fig. 6, the resonantly stabilized radicals C_3H_3 mole fraction increases by 7 % in FBA, illustrating the importance of acetylene pathways in their formation. The maximum mole fraction of C_4H_6 decreases by 4 %, denying the use of $C_2 + C_2$ routes for their formation. No significant change has been recorded for C_5H_4 mole fraction.

Fig. 7 shows that cyclopentadiene is present in relatively high concentration in both flames. C_5H_6 reaches a high at 6.6 mm of the burner and its 12 % maximum mole fraction decrease, observed in FBA, illustrates dependence of its production pathways on C_6H_6. The precocity and high value of C_5H_6 maxima suggest that its production should be performed through benzene oxidation process. Since Frank and al. (1994) have identified:

$$C_6H_5O \rightarrow c C_5H_5 + CO \qquad \text{(R. 3)}$$

as the only or the major decomposition channel of phenoxy radical at high temperature, which is formed by benzene oxidation, these observations are coherent. cC_5H_5 is the resonantly stabilized cyclopentadienyl radical, involved in naphthalene or phenanthrene production, through reactions:

$$c C_5H_5 + c C_5H_5 \rightarrow C_{10}H_8 + H + H \qquad \text{(R. 4)}$$

$$\text{Indenyl} + c C_5H_5 \rightarrow \text{Phenanthrene} + H + H \qquad \text{(R. 5)}$$

Polyacetylenic C_6H_2 mole fraction behaves as C_4H_2 in FBA. An increment of 5 % is recorded for maximum mole fraction of C_5H_8 and C_7H_8 showing importance of C_2 routes in their formation

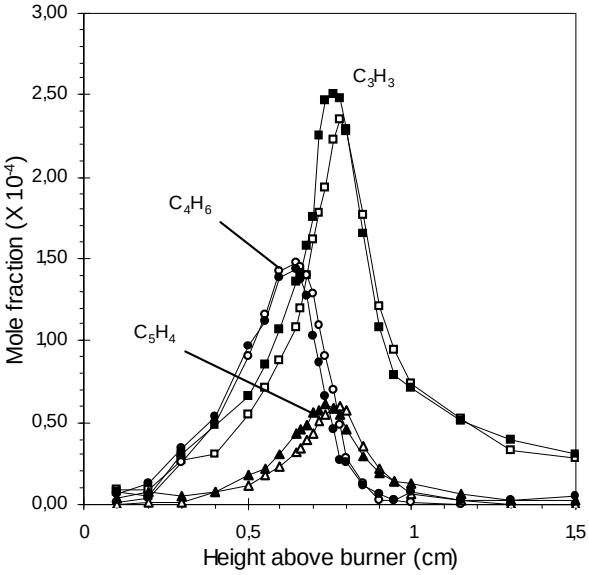

Figure 6 (symbols : empty = FB, full = FBA)

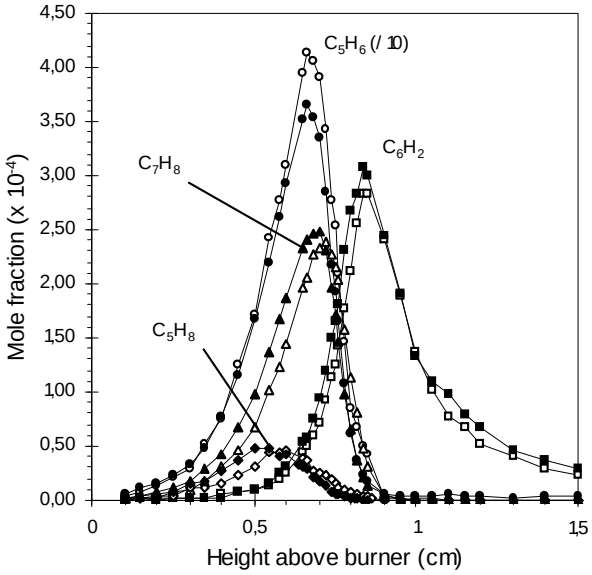

Figure 7 (symbols : empty = FB, full = FBA)

In Fig. 8, the maximum mole fraction of C_6H_6O, located close to the burner (5.8 mm) in regard of other compounds, do not critically change in FBA. This observation could be explained by the mole fraction increase of C_7H_{10} which has the same mass than C_6H_6O. C_6H_4 and C_6H_8 maximum mole fraction increase by 14 % and 6 % respectively in FBA, showing dependence of their production routes on acetylene. No significant change is recorded for C_7H_6 compound.

Fig. 9 shows that two HACA intermediate species, phenylacetylene (C_8H_6) and naphthalene ($C_{10}H_8$), maximum mole fraction increase by 17 % and 15 % in FBA, respectively. These observations show the high dependence of naphthalene formation on acetylene pathways, such as the HACA route through reactions:

$$C_6H_5 + C_2H_2 = C_8H_6 + H \quad \text{(R. 6)}$$
$$C_8H_6 + H = C_8H_5 + H_2 \quad \text{(R. 7)}$$
$$C_8H_5 + C_2H_2 = C_{10}H_7 \quad \text{(R. 8)}$$
$$C_{10}H_7 + H = C_{10}H_8 \quad \text{(R. 9)}$$

At its maximum, C_8H_8 mole fraction decreases significantly in FBA, showing that acetylene routes are not mainly involved in its formation.

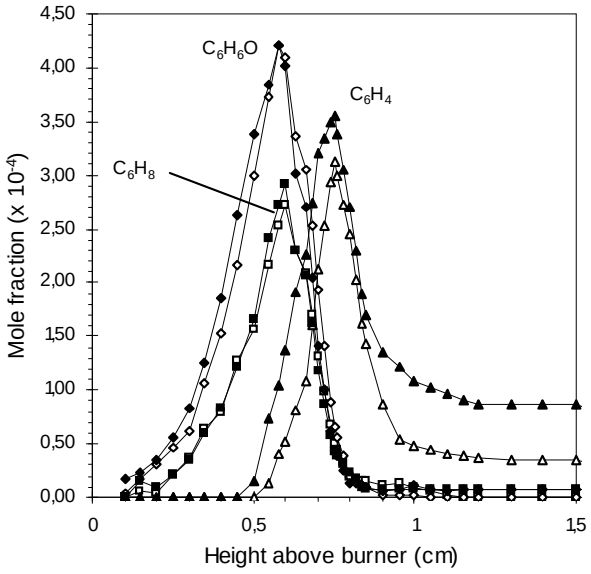

Figure 8 **(symbols : empty = FB, full = FBA)**

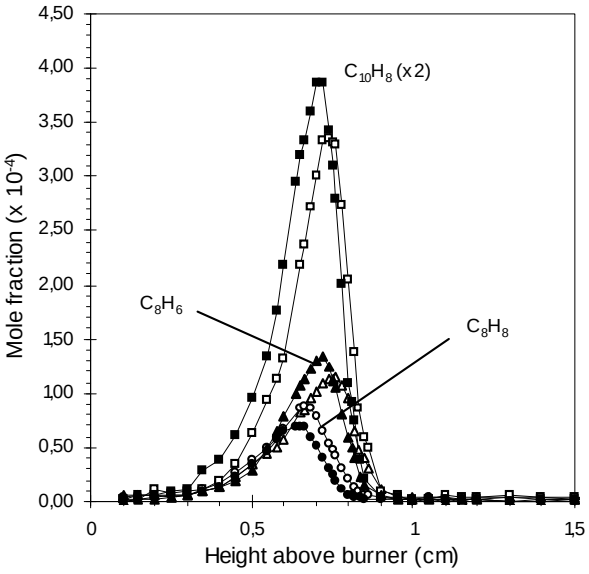

Figure 9 **(symbols : empty = FB, full = FBA)**

In Fig. 10, diethynylbenzene ($C_{10}H_6$) and methylnaphthalene ($C_{11}H_{10}$) maximum mole fractions decrease by 14 % and 11 % respectively, showing the dependence of their production pathways on benzene.

Fig. 11 shows that biphenyl ($C_{12}H_{10}$) maximum mole fraction decreases by 8 % in FBA. Since $C_{12}H_{10}$ is formed by benzene – phenyl additions (Fig. 12), smallest benzene availability in FBA explains this observation. Production of $C_{13}H_{10}$ seems slightly stimulated in FBA.

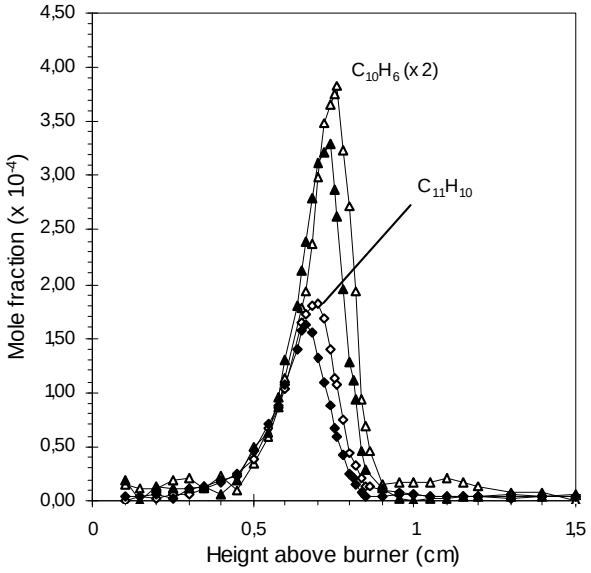

Figure 10 **(symbols : empty = FB, full = FBA)**

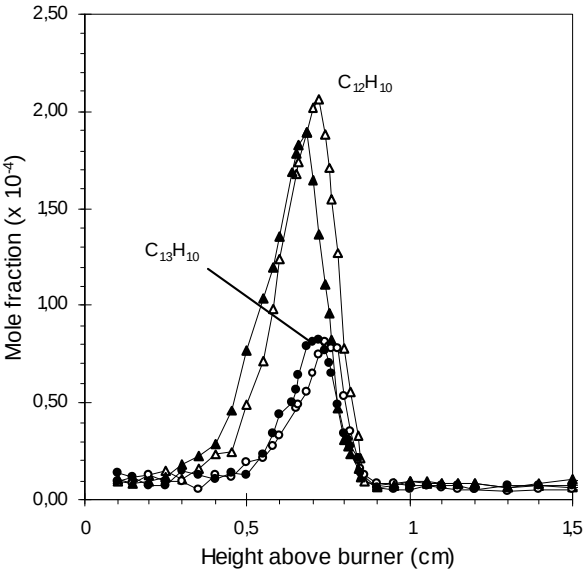

Figure 11 **(symbols : empty = FB, full = FBA)**

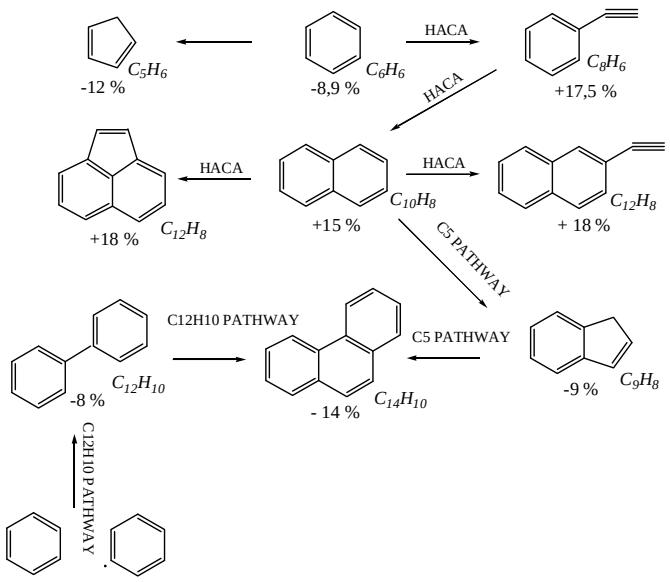

Figure 12 : Phenanthrene formation pathways. Percentages represent variation of maximum mole fraction in FBA, compared with the FB reference flame.

In Fig. 13, acenaphthylene ($C_{12}H_8$) maximum mole fraction increases by 18 %. Therefore, the formation of this chemical species involves acetylene depending routes, such as the HACA pathway. Indene (C_9H_8) maximum decreases by 9 % in FBA. Phenanthrene ($C_{14}H_{10}$) is produced in lower concentration in FBA. The 14 % decrease of its mole fraction maximum indicates that its production route does not mainly involve an H abstraction and an acetylene addition process on naphthalene.
One can assume that the phenanthrene formation is essentially performed either by a HACA route on biphenyl ($C_{12}H_{10}$) or through a cyclopentadienyl (cC_5H_5) addition on indenyl (C_9H_7) radical (R. 5), as illustrate in Fig. 12.

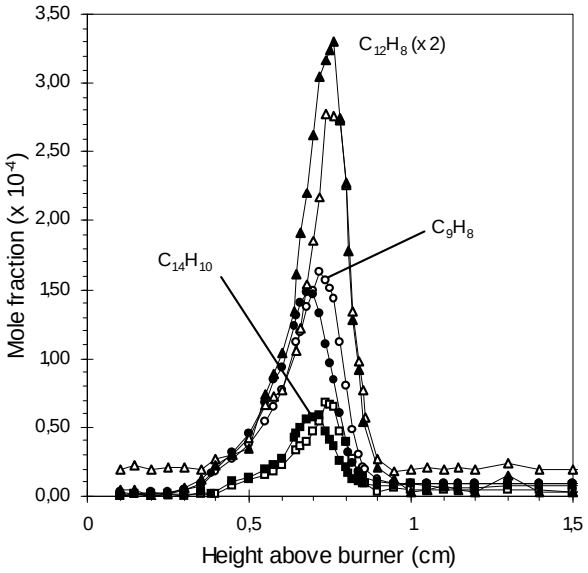

Figure 13 (symbols : empty = FB, full = FBA)

Modelling

Previously, Dias (2003) has developed a reaction mechanism validated against premixed rich $C_2H_4/O_2/Ar$ flames (ϕ = 2.25 and 2.50) which describes in detail the formation of soot precursors (until naphthalene) and the main pathways involving benzene. Its reliability has been already extended to various hydrocarbon burning flames at several equivalence ratios: for less rich ethylene flames (ϕ = 1.0 to 2.0) as well as for rich methane (CH_4), acetylene (C_2H_2) and ethane (C_2H_6) flames in the equivalence ratio range from ϕ = 1.0 to 2.0 (Dias et al., 2003). The detailed mechanism involving 78 chemical species with the naphthalene as the heaviest and 402 elementary reactions has been slightly modified to taking into account recent kinetic parameters.

The aim of this section is to check the reliability of this model in rich premixed benzene flames, when the initial hydrocarbon is the first aromatic ring. Moreover, this reaction mechanism has to be extended to model heavier polycyclic aromatic hydrocarbons detected in these two rich benzene flames, until the $C_{18}H_{10}$ species.

Some experimental and simulated mole fraction profiles are presented in Figs. 14, 15, 16 and 17, for main species (C_6H_6, O_2, CO, CO_2, H_2 and H_2O) in FB, for C_2H_2, C_3H_3, C_9H_8 and $C_{10}H_8$, respectively in FB and FBA flames. Symbols represent experimental while lines show simulated data.

Fig. 14 shows the modelling of mole fraction profiles for the main species in the benzene flame FB (without addition of acetylene). We must underline the good agreement between experimental and simulated results.

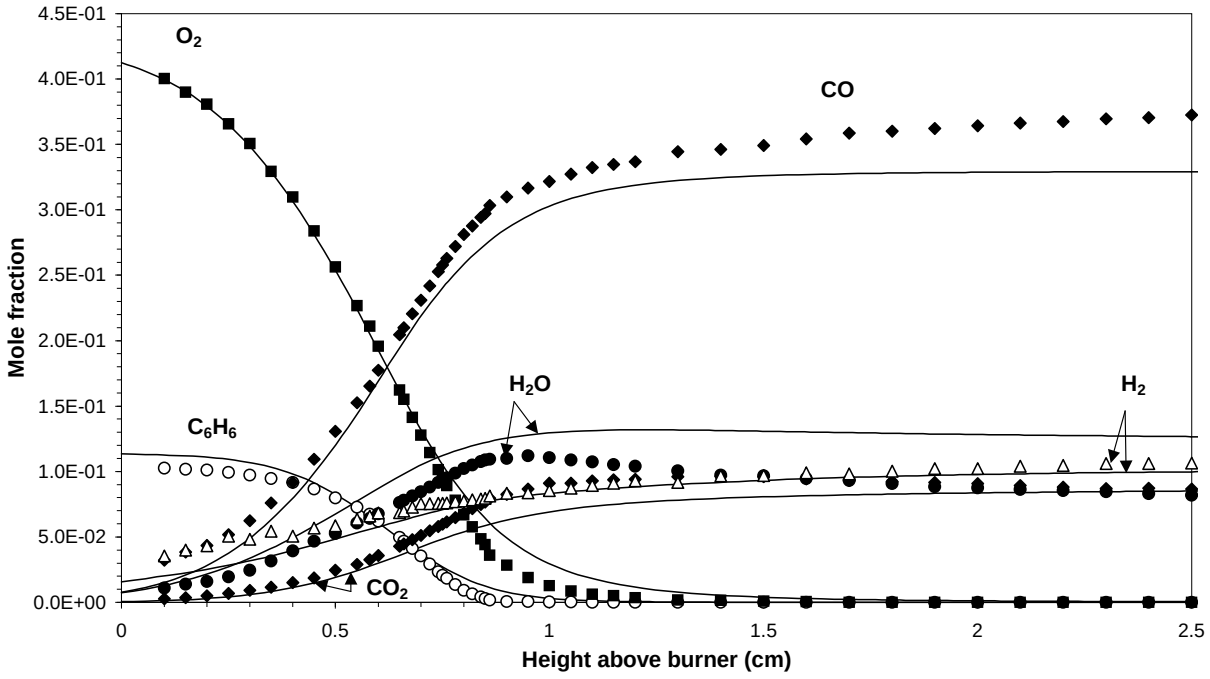

Figure 14 : Experimental and simulated mole fraction profiles of C_6H_6, O_2, CO, CO_2, H_2 and H_2O in FB

Fig. 15 shows simulated and experimental mole fraction profiles of C_2H_2 and C_3H_3 in both FB and FBA flames.
The shape of acetylene profiles is different according to the initial composition of the flame because in FBA, C_2H_2 is a reactant. In this last case, we notice that the experimental profile of C_2H_2 indicates the formation then its consumption. We can suggest that C_2H_2 is produced faster from the degradation of benzene than it is consumed. But, the mechanism indicates a consumption of the acetylene at first, then only its formation (from the oxidation of the benzene) and finally a consumption in the burned gases region.
The difference between both profiles indicates that the kinetic model underestimates the reaction rate of production of the acetylene from the benzene, or overestimates the reaction rate of consumption of the acetylene in the flame front. A detailed analysis of reaction pathways will give an answer to this observation.
In the FB flame, the shape of the C_2H_2 profile corresponds well to that obtained experimentally, with however a shift towards the zone of post-combustion which can be ascribed to a temperature profile displaced downwards.
For both flames, we can underline that the kinetic mechanism overestimates the C_2H_2 mole fraction in the burned gases.

The experimental concentration of the propargyl radical (C_3H_3) is very slightly higher in the FBA flame than in the FB flame, with a production slightly earlier in the flame front (Fig. 15). The mechanism reports these two observations. However for both flames of benzene, the simulated profiles are shift towards burned gases with a too slow consumption in this zone compared to the experimental results. The presence of acetylene in fresh gases (FBA) does not induce any difference with the neat benzene (FB) flame as long as for the experiment that for the simulation.

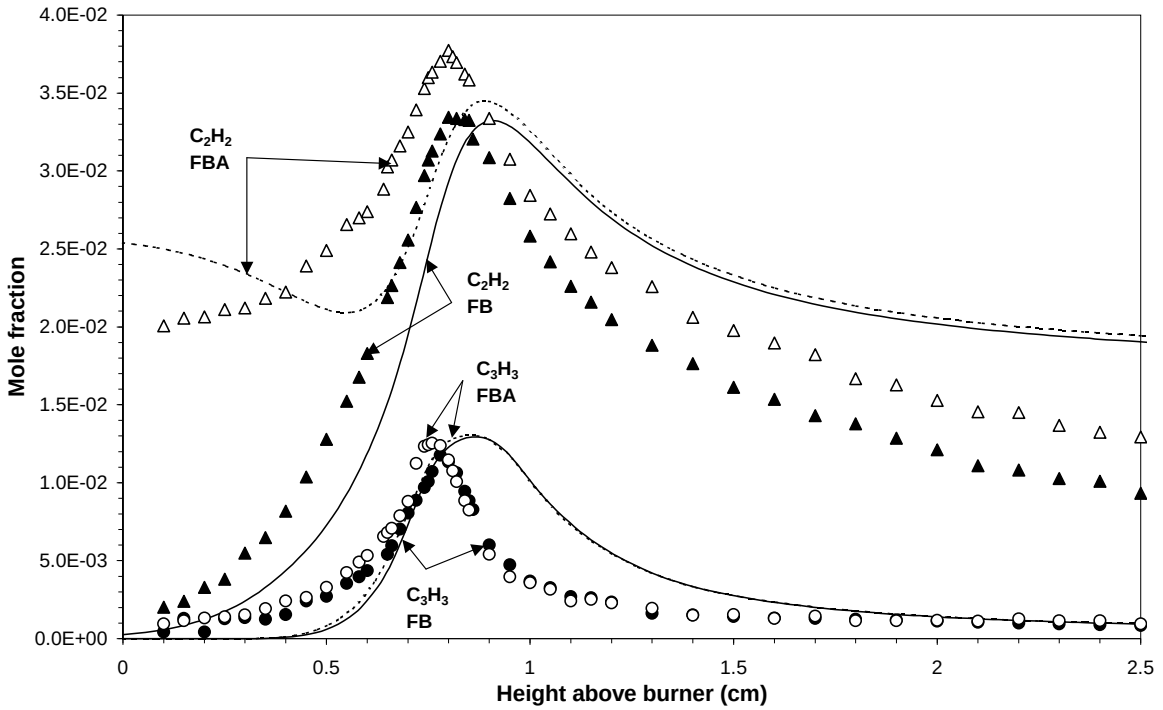

Figure 15: Experimental and simulated profiles of C_2H_2 and C_3H_3 in both flames : FB and FBA

However for species heavier than benzene (main reactant of these flames), the simulation overestimates strongly mole fraction values. Such results may proceed from the fact that the kinetical schema does not involve larger species than naphthalene. In fact their further consumptions are not well estimated.

Conclusion

The comparison of a benzene-oxygen-argon with a benzene-acetylene-oxygen-argon flames, both sooting with an equivalence ratio of two, have allowed us to evaluate more precisely the role of C_2H_2 in hydrocarbons and PAH production. If acetylene presence in fresh gases does not largely alter main chemical species profiles, the incidence on intermediate compounds is more significant. Analysis of measured profiles provides two important clues on PAH formation.

Firstly, since cyclopentadiene mole fraction decreases in FBA and HACA intermediates species maximum mole fractions increase, in benzene flames the naphthalene formation should be performed through the Hydrogen Abstraction C_2H_2 Addition route. Secondly, the drop down measured in phenanthrene maximum mole fraction indicates that its production should mainly be achieved either through the biphenyl or the cyclopentadienyl pathways. Moreover these experimental facts, results will be an interesting inspiration source for PAH production simulation. For example, the no curving down of C_2H_2 profile, observed in FBA, before it reaches a high, will be helpful to improve actual C_2H_2 simulations in rich hydrocarbons flames.

Whereas this preliminarily molecular beam mass spectrometry analysis provides interesting clues on PAH formation, it should be completed by a gas chromatography investigation, in further works, in order to separate mass isomers and study heavier PAH.

Before elaborating the complete mechanism modeling the flames of benzene until the heaviest species ($C_{18}H_{10}$), we have analysed the results of the simulation by the original mechanism (Dias, 2003), up to the naphthalene ($C_{10}H_8$). A certain kinetic incoherence for some large species emerges from it and this initial mechanism must be corrected before being completed to model all the present species in both flames, FB and FBA.

Acknowledgements

The authors are very grateful to the Ministère de la Région Wallone for the financial support (Visa n° 05/335552).

References

Bittner, J.D. and Howard, J.B. (1981), *Proc. Combust. Instit.*, 18, 1105.

Castaldi, M.J., Marinov, N.M., Melius, C.F., Senkan, S.M., Pitz, W.J. and Westbrook, C.K. (1996), *Proc. Combust. Instit.*, 26, 693.

Defoeux, F., Dias, V., Renard, C., Van Tiggelen, P.J. and Vandooren, J. (2005), *Proc. Combust. Instit.*, 30 1407.

Dias, V. (2003) Etude de la formation des précurseurs des suies dans les flammes riches prémélangées d'éthylène, *PhD Thesis Université catholique de Louvain,* Belgium.

Dias, V., Renard, C., Van Tiggelen, P.J. and Vandooren, J. (2003), *Proc. of European Combustion Meeting*, p.221.

Dias, V., Renard, C., Van Tiggelen, P.J. and Vandooren, J. (2004), *Combust. Sci. and Technol.*, 176, 1419.
Dockery, D.W., Pope, C.A., Xu, X., Spengler, J.D., Ware, J.H., Fay, M.E., Ferris, B.G., Speizer, F.E. (1993), *New Engl. J. Med.*, 329, 1753.
Frank, P., Herzler, J., Just, Th. and Wahl, C. (1994), *Proc. Combust. Instit.*, 25, 833.
Frenklach, M., Clary, D.W., Gardiner, W. C. and Stein, S. E. (1984), *Proc. Combust. Instit.*, 20, 887.
Frenklach, M., Clary, D.W., Gardiner, W. C. and Stein, S. E. (1986), *Proc. Combust. Instit.*, 21, 1067.
Frenklach, M. and Warnatz, J. (1987), *Combust. Sci. and Technol.*, 51, 265.
Frenklach, M. and Wang, H. (1990), *Proc. Combust. Instit.*, 23, 1559.
Frenklach, M. (2002), *Phys. Chem. Chem. Phys.*, 4, 2028.
Marinov, N.M., Pitz, W.J., Westbrook, C.K., Castaldi, M.J. and Senkan, S.M. (1996), *Combust. Sci. and Technol.*, 116-117, 211.
Marinov, N.M., Pitz, W.J., Westbrook, C.K., Vincitore, A.M., Castaldi, M.J. and Senkan, S.M. (1998), *Combust. Flame*, 114, 192.
Rasmussen, C.L., Skjøth-Rasmussen, M.S., Jensen, A.D. and Glarborg, P. (2005), *Proc. Combust. Instit.*, 30, 1023.
Richter, H., Grieco, W.J. and Howard, J.B. (1999), *Combust. Flame*, 119, 1.
Siegmann, K. and Siegmann, H.C. (1998) Current problems in condensed matter, Plenum Press, New York, pp. 143-160.
Vandooren, J., Branch, M.C. and Van Tiggelen, P.J. (1992), *Combust. Flame*, 90, 247.
Wang, H. and Frenklach, M. (1997), *Combust. Flame*, 110, 173.
Warnatz, J. (1984), *Proc. Combust. Instit.*, 20, 845.

Theoretical Determination of Thermodynamic Data of Precursors of the First Aromatic Ring in Flames

Xavier Lories
Laboratoire de Physico-Chimie de la Combustion
Université Catholique de Louvain

IEA-29TLM 2007, Gembloux

Good ring formation modelling needs

- Good understanding of the mechanisms
- Accurate thermodynamic data
- Reliable rate constants

Good ring formation modelling needs

- Good understanding of the mechanisms
- **Accurate thermodynamic data**
- Reliable rate constants

Accuracy of energies

- Limitations due to computer costs :
- Size of the basis set
- Amount of electron correlation

G3B3

Basis set

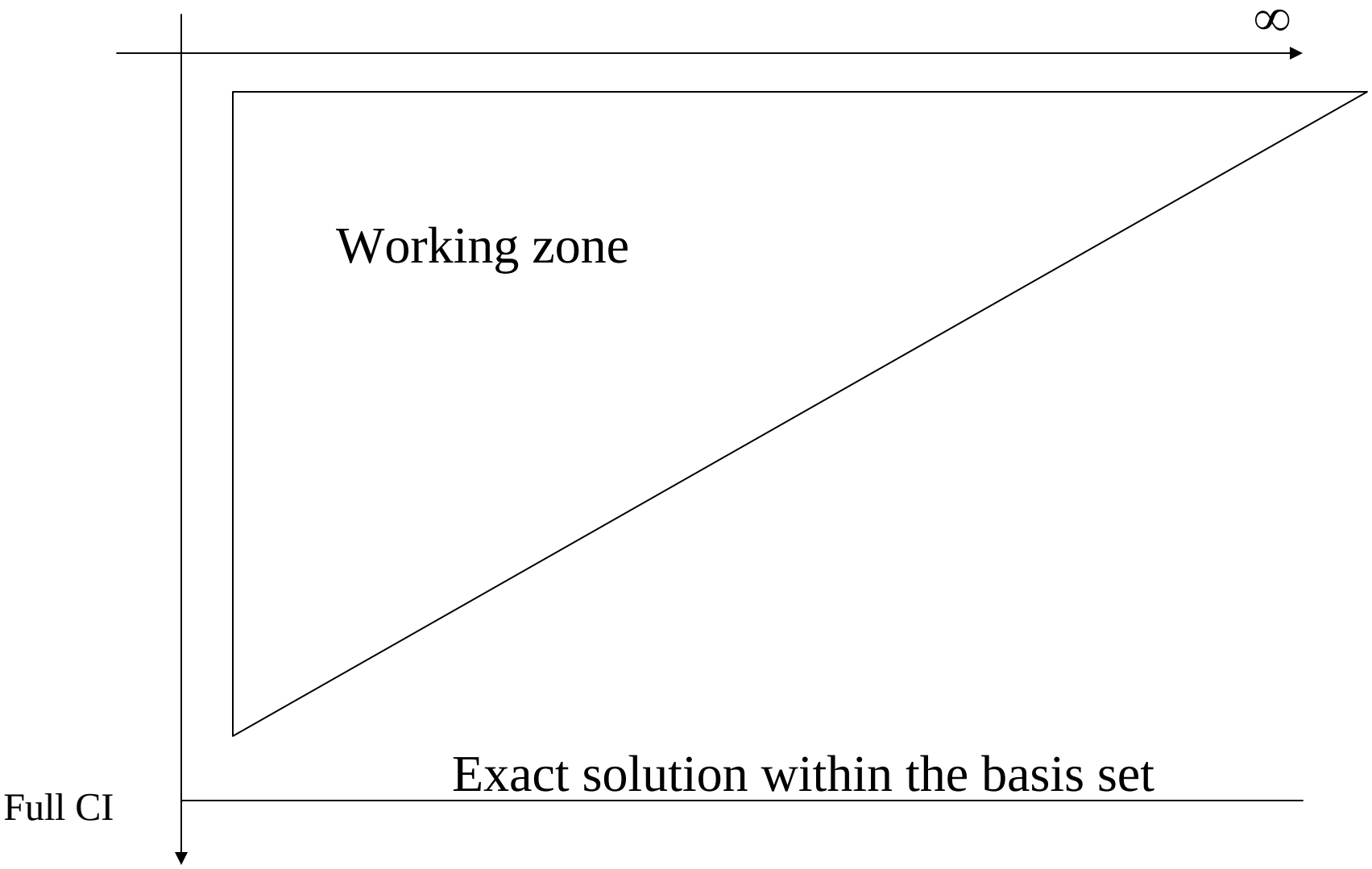
∞
Working zone
Exact solution within the basis set
Full CI
Electron correlation

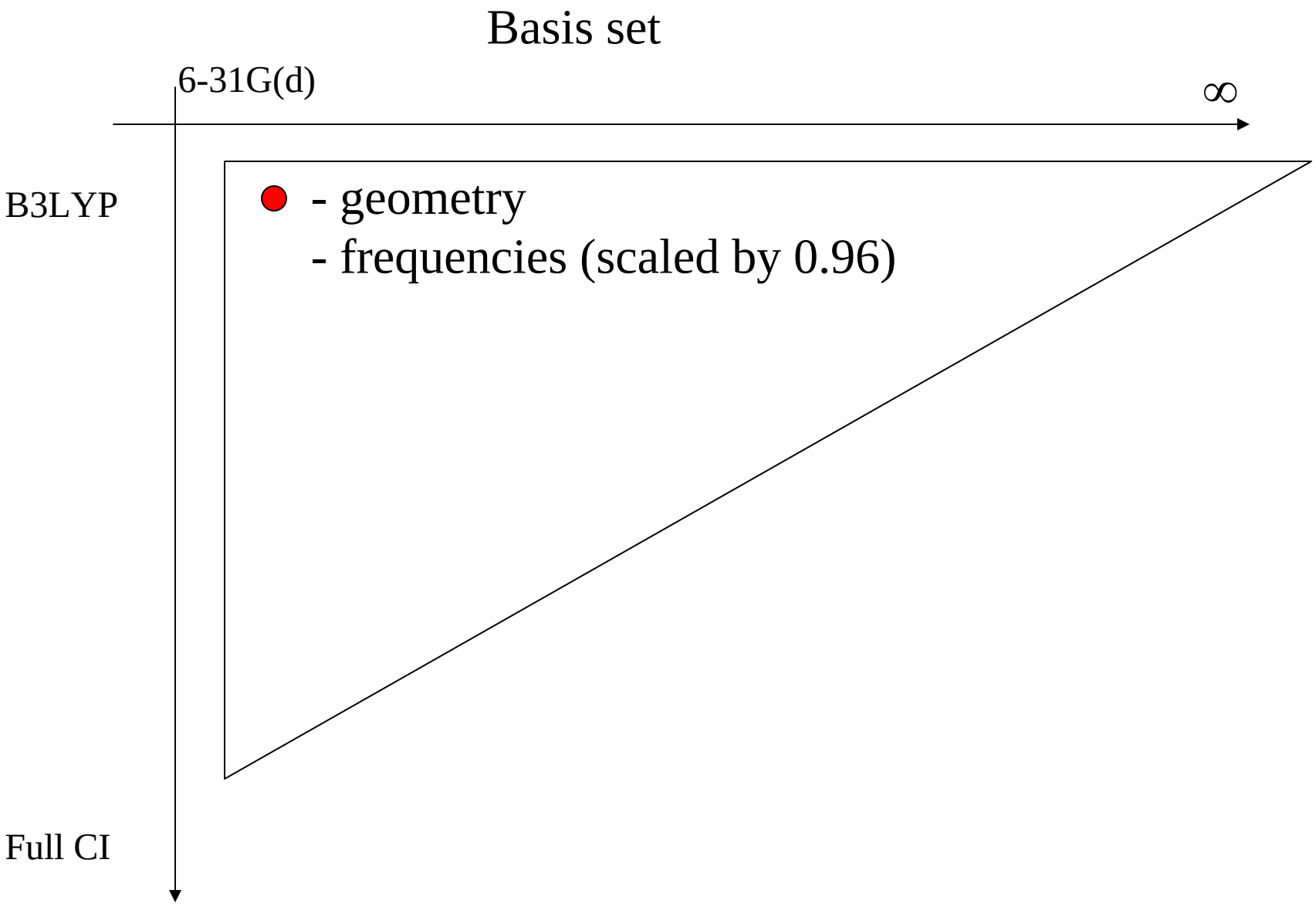
Basis set
6-31G(d)
∞
B3LYP
- geometry
- frequencies (scaled by 0.96)
Full CI
Electron correlation

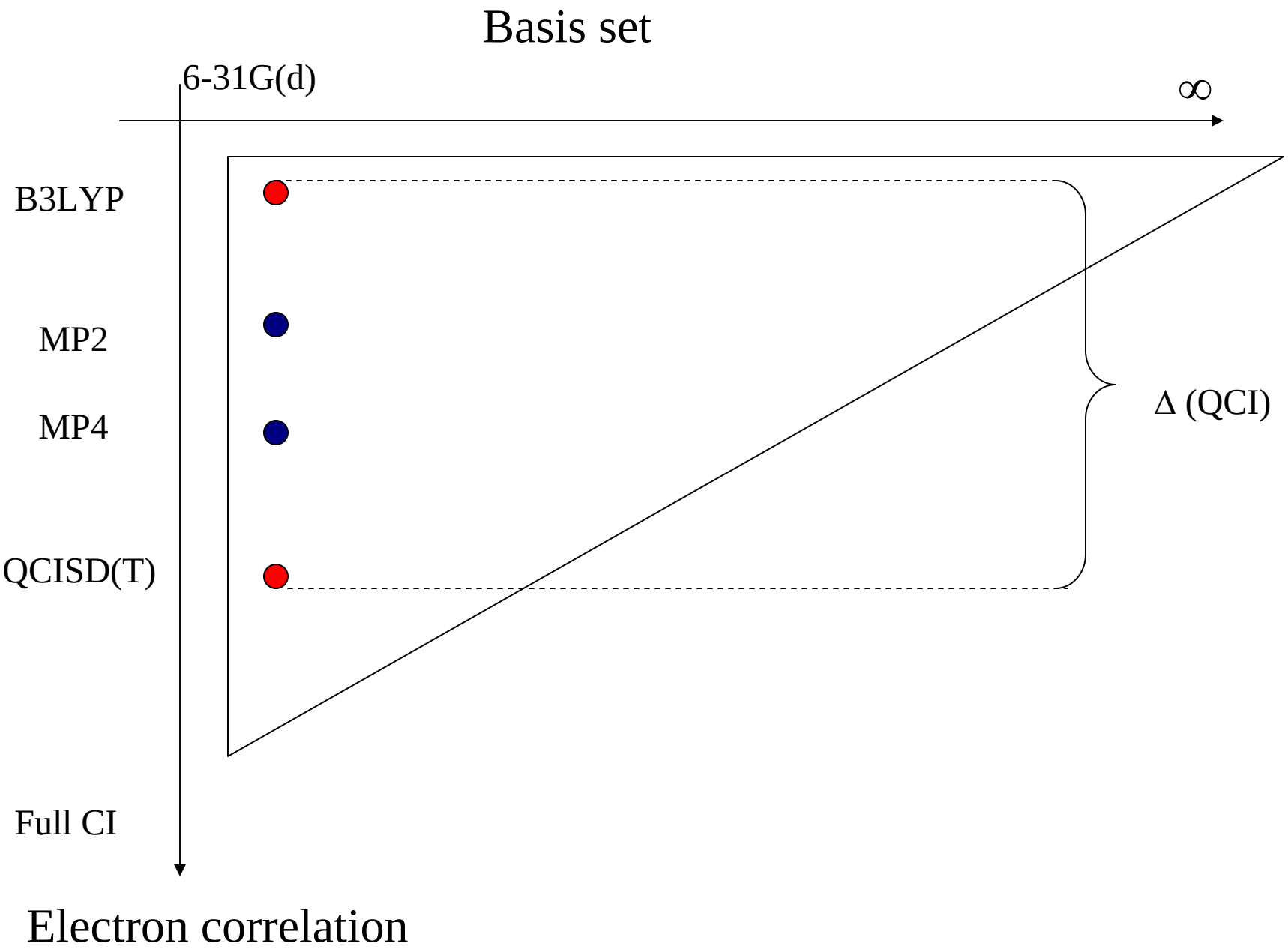
Basis set
6-31G(d)
∞
B3LYP
MP2
MP4
QCISD(T)
Full CI
Δ (QCI)
Electron correlation

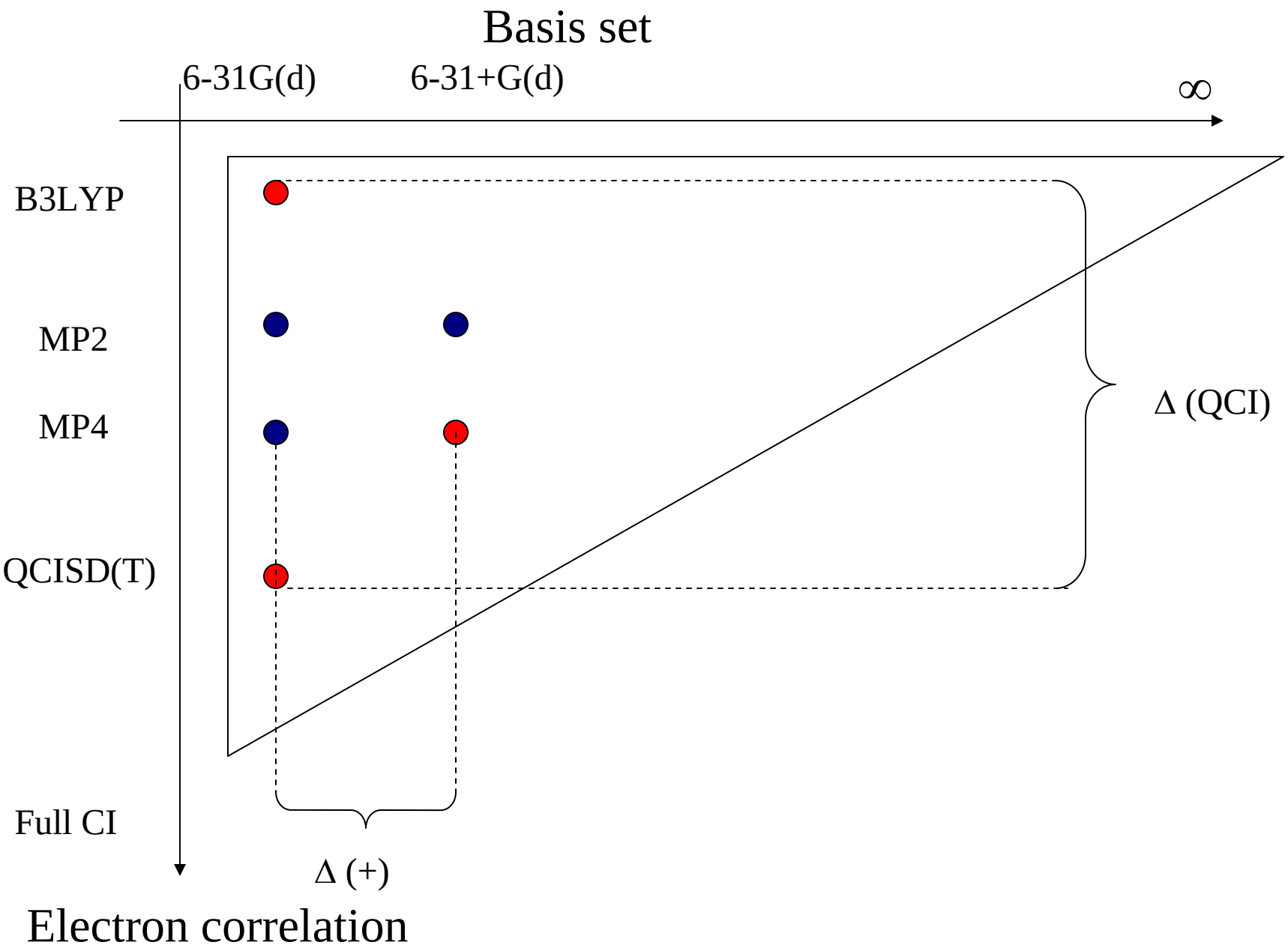
Basis set
6-31G(d)
6-31+G(d)
∞
B3LYP
MP2
MP4
QCISD(T)
Full CI
Δ (QCI)
Δ (+)
Electron correlation

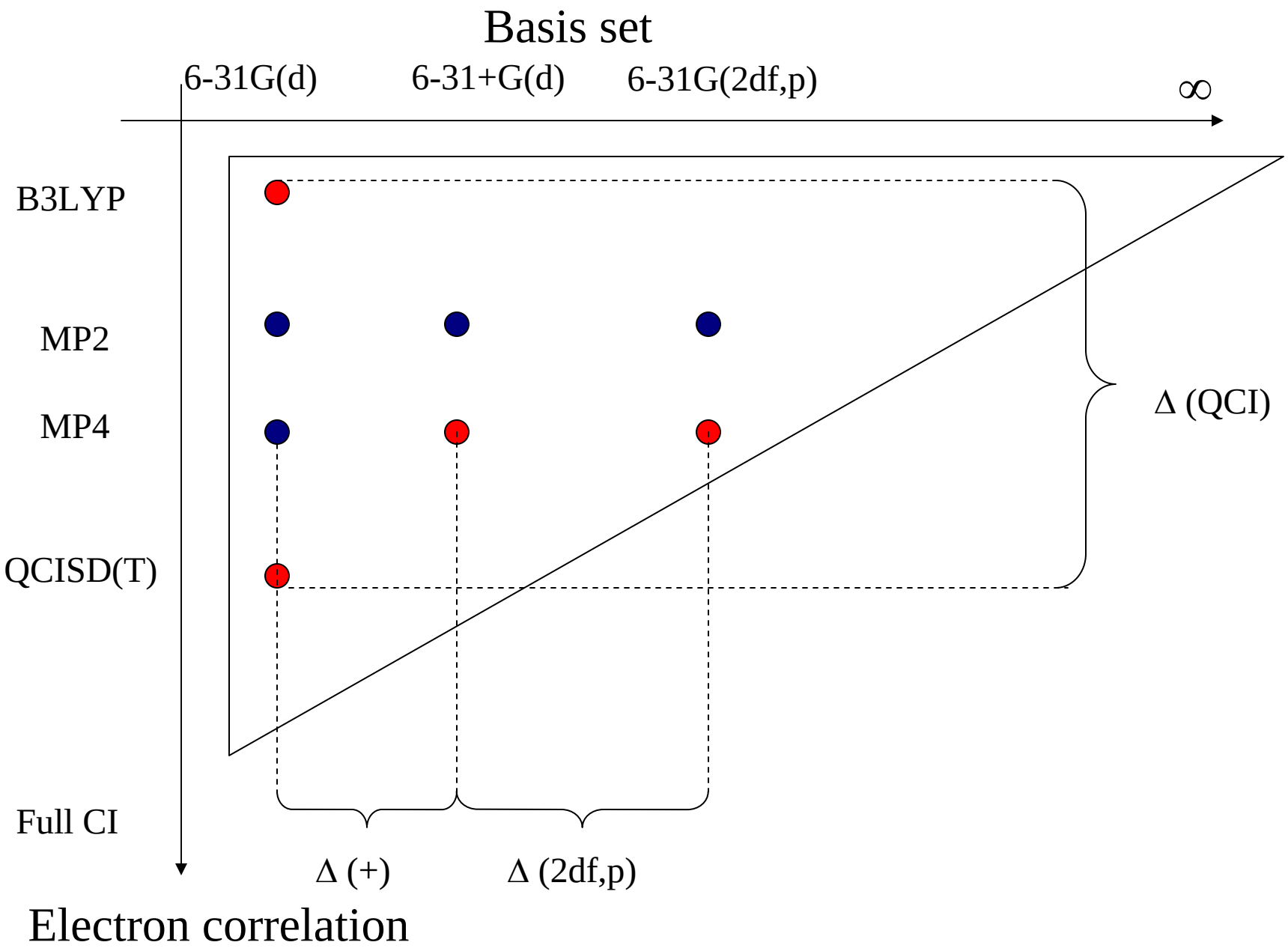
Basis set
6-31G(d)
6-31+G(d)
6-31G(2df,p)
∞
B3LYP
MP2
MP4
QCISD(T)
Full CI
Δ (QCI)
Δ (+)
Δ (2df,p)
Electron correlation

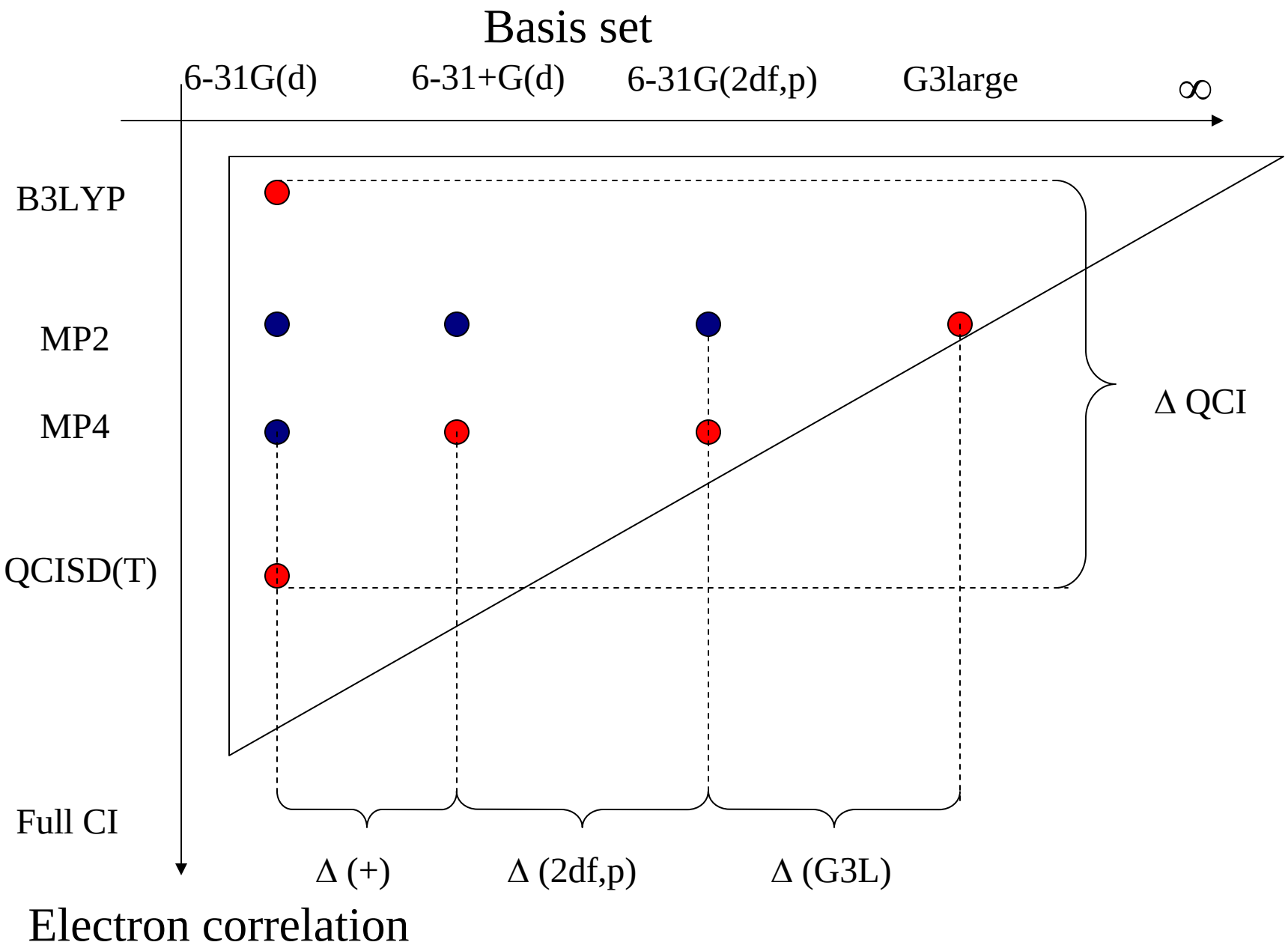
Basis set
6-31G(d)
6-31+G(d)
6-31G(2df,p)
G3large
∞
B3LYP
MP2
MP4
QCISD(T)
Full CI
Δ QCI
Δ (+)
Δ (2df,p)
Δ (G3L)
Electron correlation

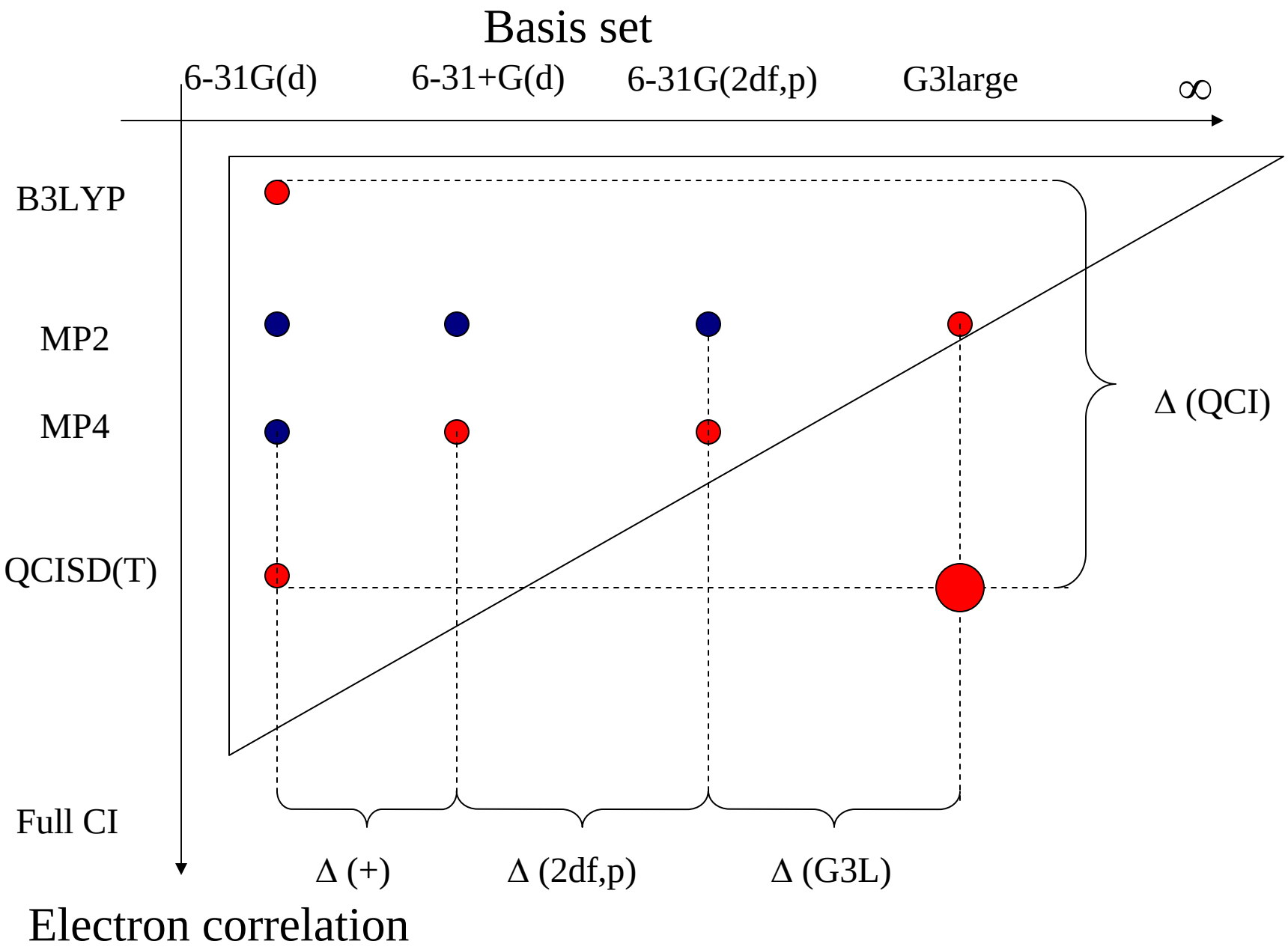
Basis set
6-31G(d)
6-31+G(d)
6-31G(2df,p)
G3large
∞
B3LYP
MP2
MP4
QCISD(T)
Full CI
Δ (QCI)
Δ (+)
Δ (2df,p)
Δ (G3L)
Electron correlation

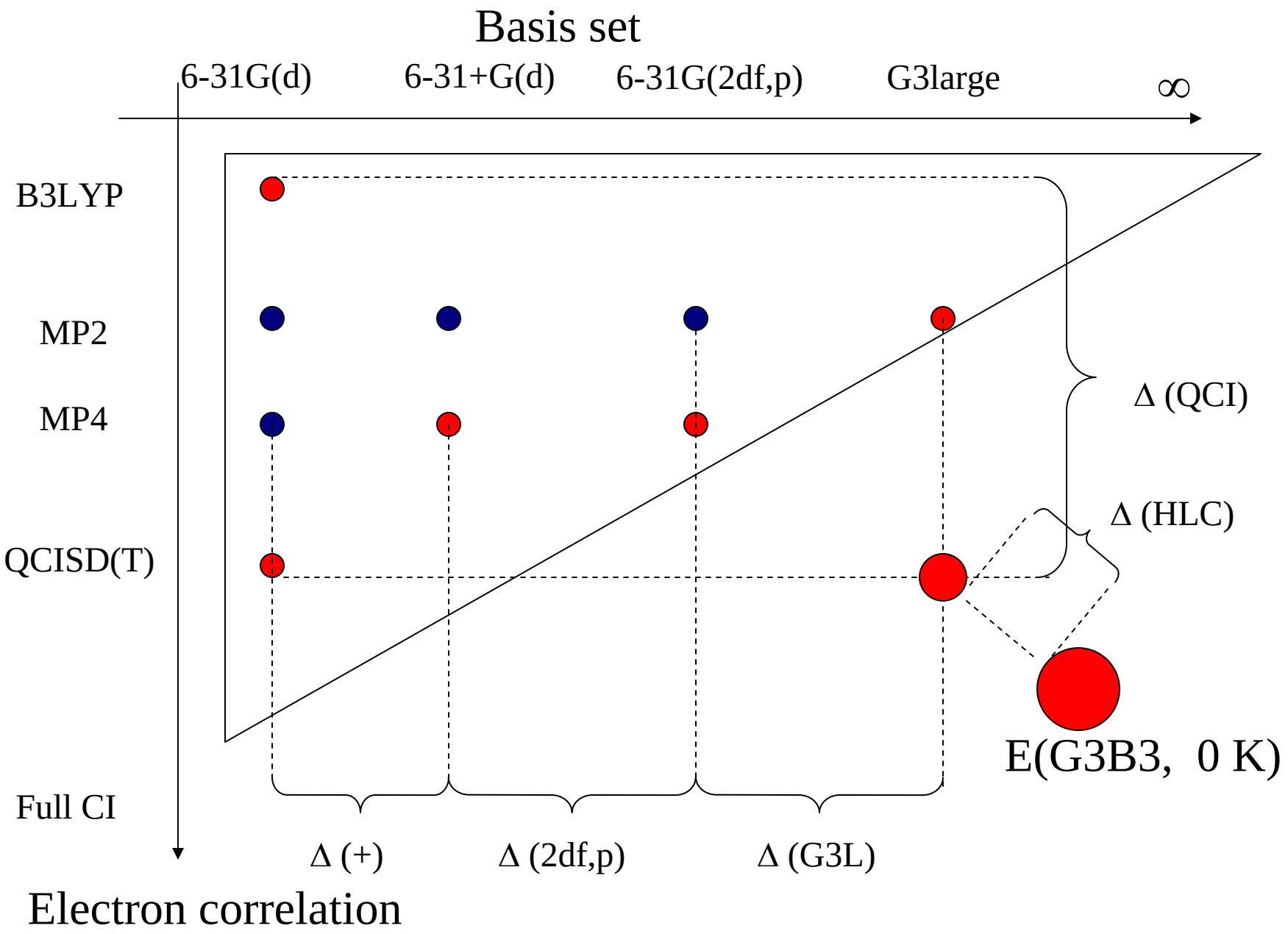
Basis set
6-31G(d)
6-31+G(d)
6-31G(2df,p)
G3large
∞
B3LYP
MP2
MP4
QCISD(T)
Full CI
Δ (QCI)
Δ (HLC)
E(G3B3, 0 K)
Δ (+)
Δ (2df,p)
Δ (G3L)
Electron correlation

Heats of formation

- 3 Methods:

- Atomization reactions (M1)
- Hydrogenation reactions (M2)
- Isodesmic reactions (M3)

Why three methods ?

- Find the most appropriate

  → Hydrocarbon test set

- Compare results

Atomization reactions (M1)

Pour C_nH_m : $C_nH_m \rightarrow nC + mH$

$$\sum D_0 = n\varepsilon_0(C, 0K) + m\varepsilon_0(H, 0K) - \varepsilon_0(C_nH_m, 0K)$$

$$\Delta H_f^o(C_nH_m, 0K) = n\Delta H_f^o(C, 0K) + m\Delta H_f^o(H, 0K) - \sum D_0$$

$$\Delta H_f^o(C_nH_m, 298K) = \Delta H_f^o(C_nH_m, 0K)$$
$$+ \left[H(C_nH_m, 298K) - H(C_nH_m, 0K)\right]$$
$$- n\left[H(C, 298K) - H(C, 0K)\right] - m\left[H(H, 298K) - H(H, 0K)\right]$$

Hydrogenation reactions

Pour C_nH_m : $C_nH_m + \frac{(4n-m)}{2} H_2 \rightarrow nCH_4$

References:

$\Delta H_f^o(CH_4) = -17{,}89\ kcal.mol^{-1}$

$\Delta H_f^o(H_2) = 0\ kcal.mol^{-1}$

Isodesmic reactions

- Conservation of errors
- Use of Bond Separation Reactions

$$\Delta H_f^o(CH_4) = -17{,}89\ kcal.mol^{-1}$$

$$\Delta H_f^o(C_2H_2) = 54{,}19\ kcal.mol^{-1}$$

$$\Delta H_f^o(C_2H_4) = 12{,}54\ kcal.mol^{-1}$$

$$\Delta H_f^o(C_2H_6) = -20{,}04\ kcal.mol^{-1}$$

Example of isodesmic reaction

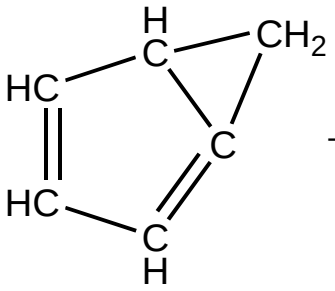

+ 8 CH_4 → 5 C2H6 + 2 C2H4

5 C-C bonds

2 C=C bonds

6 C-H bonds

32 C-H bonds

5 C-C bonds

30 C-H bonds

2 C=C bonds

8 C-H bonds

M3-2 and M3-3 methods

- M3-2 introduction of cyclopropane into reference set
- M3-3 introduction of cyclobutane in reference set

Examples of results

Compound (exp)	M1	M2	M3
Allene (45.53)	44.96	43.56	45.26
Propane (-25.02)	-24.96	-25.53	-25.09
2-butyne (34.68)	34.55	32.82	34.49
Cyclopentadiene (33.2)	32.60	30.13	32.49
Cyclobutane (6.8)	7.08	5.77	6.65
Benzene (19.82)	20.34	17.13	20.34

Units are $kcal.mol^{-1}$

Results for the test set (32 species)

	M1	M2	M3
MD	-0,47	1,35	-0,34
MAD	0,75	1,49	0,69
MAX	2,42	3,62	1,96
MIN	0,06	0,08	0,03

Units are $kcal.mol^{-1}$

MD : Mean Deviation

MAD : Mean Absolute Deviation

MAX : Maximum absolute deviation

MIN : Minimum absolute deviation

Why are M2 results so bad?

- M3 : conserves the environment

  → Cancellation of errors

- M1: Removes environment

  → Conservation of errors

- M2 : Modifies environment

  → Accumulation of errors

Results

- M1 results similar to M3 ones
- M1 and M3: high deviation for strained compounds
- Use of M3-2 and M3-3 does not improve results

Mechanisms

- C_3+C_3 : propargyl radicals recombination
- C_4+C_2
- Fulvene isomerisation

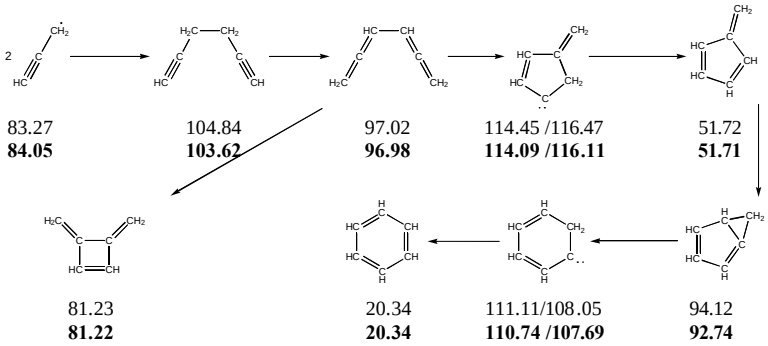

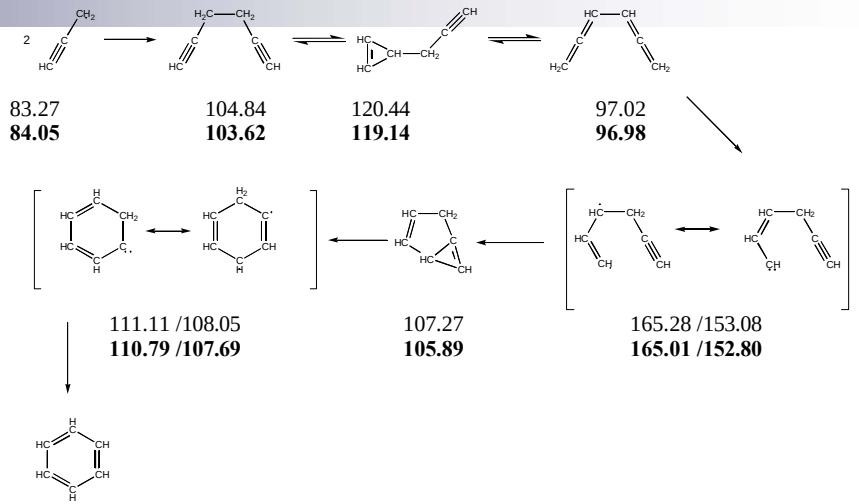

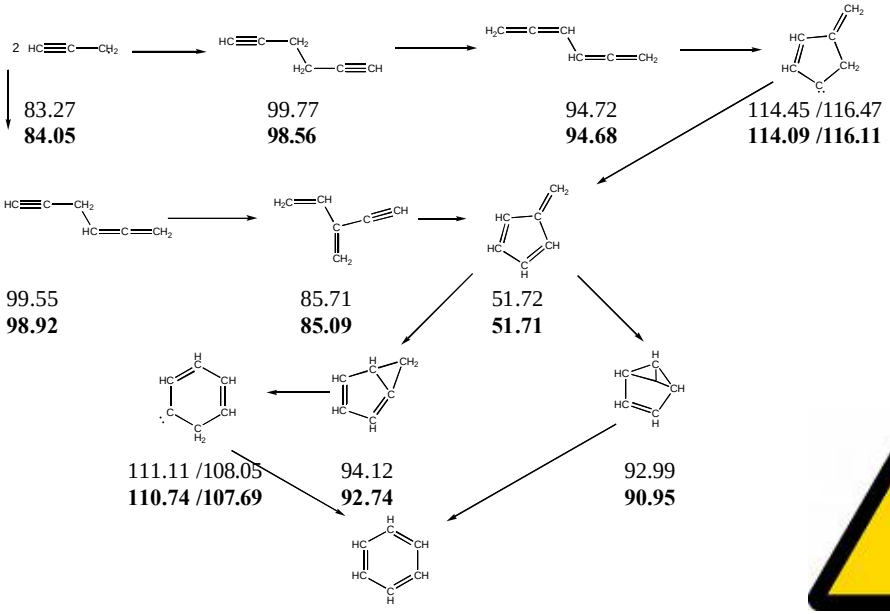

C_3+C_3 : Propargyl radicals recombination

Error on propargyl radical

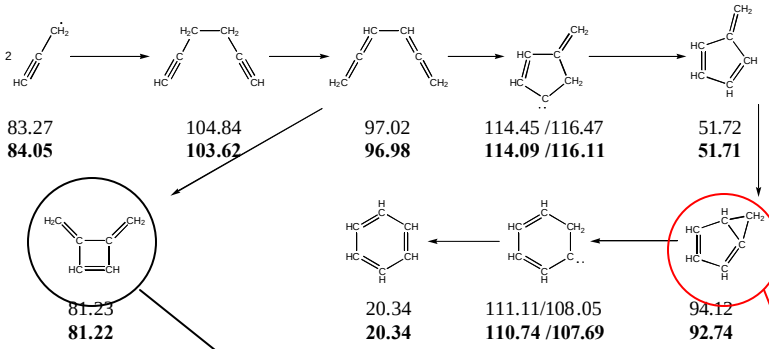
83.27
84.05
104.84
103.62
97.02
96.98
114.45 /116.47
114.09 /116.11
51.72
51.71
81.23
81.22
20.34
20.34
111.11/108.05
110.74 /107.69
94.12
92.74

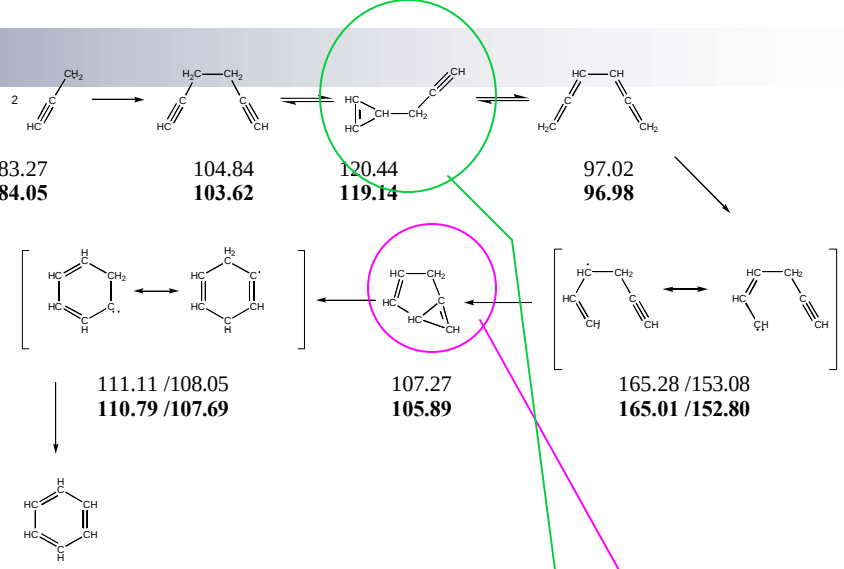
83.27
84.05
104.84
103.62
120.44
119.14
97.02
96.98
111.11 /108.05
110.79 /107.69
107.27
105.89
165.28 /153.08
165.01 /152.80

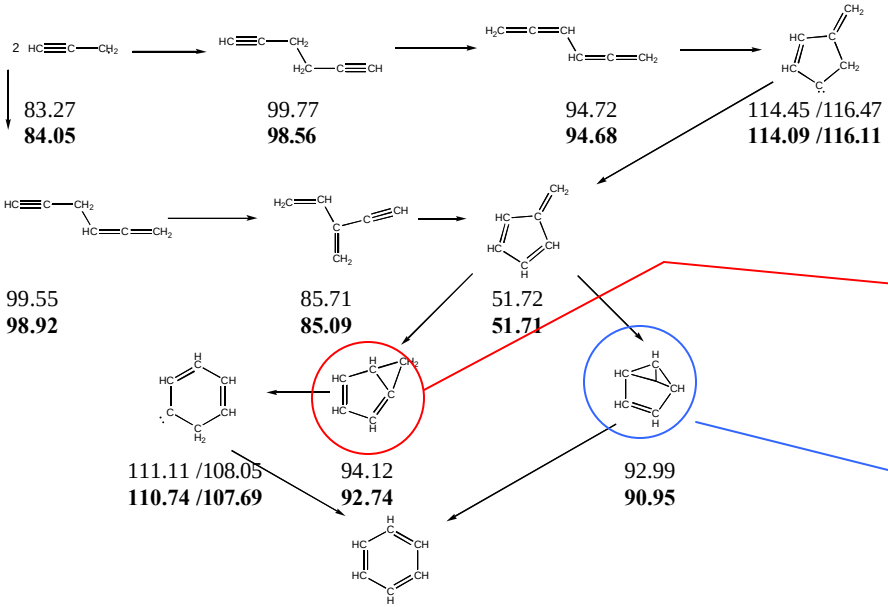
83.27
84.05
99.77
98.56
94.72
94.68
114.45 /116.47
114.09 /116.11
99.55
98.92
85.71
85.09
51.72
51.71
111.11 /108.05
110.74 /107.69
94.12
92.74
92.99
90.95

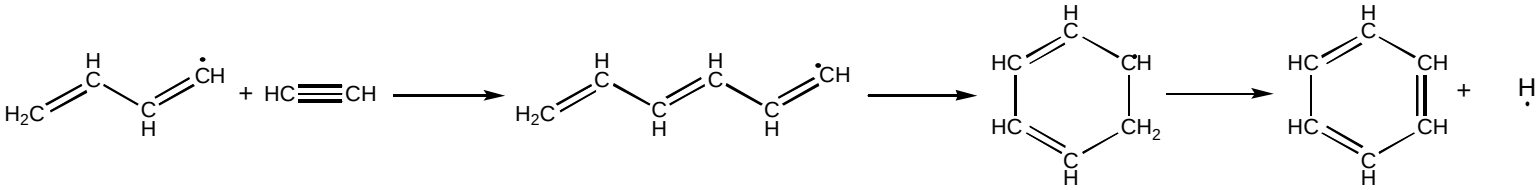

86.86	54.34	106.11	50.41	20.34	52.1
87.13	/	**106.15**	**49.77**	**20.34**	**52.3**

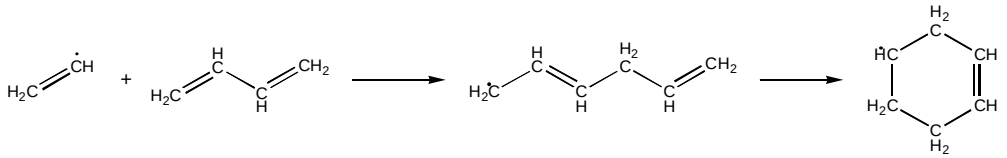

70.29	26.50	52.89	45.75	
70.79	**26.49**	**52.73**	**44.92**	

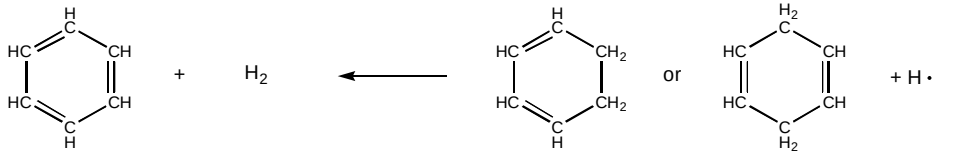

20.34	-0.41	26.10	26.18		52.1
20.34	/	**25.2**	**25.27**		**52.3**

C_4+C_2 mechanisms

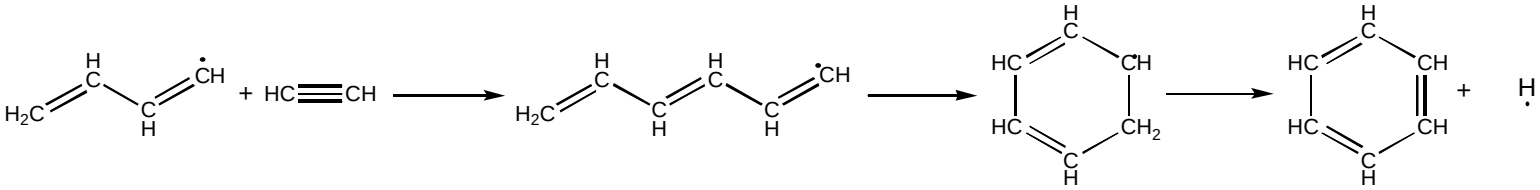

86.86	54.34	106.11	50.41	20.34	52.1
87.13	/	**106.15**	**49.77**	**20.34**	**52.3**

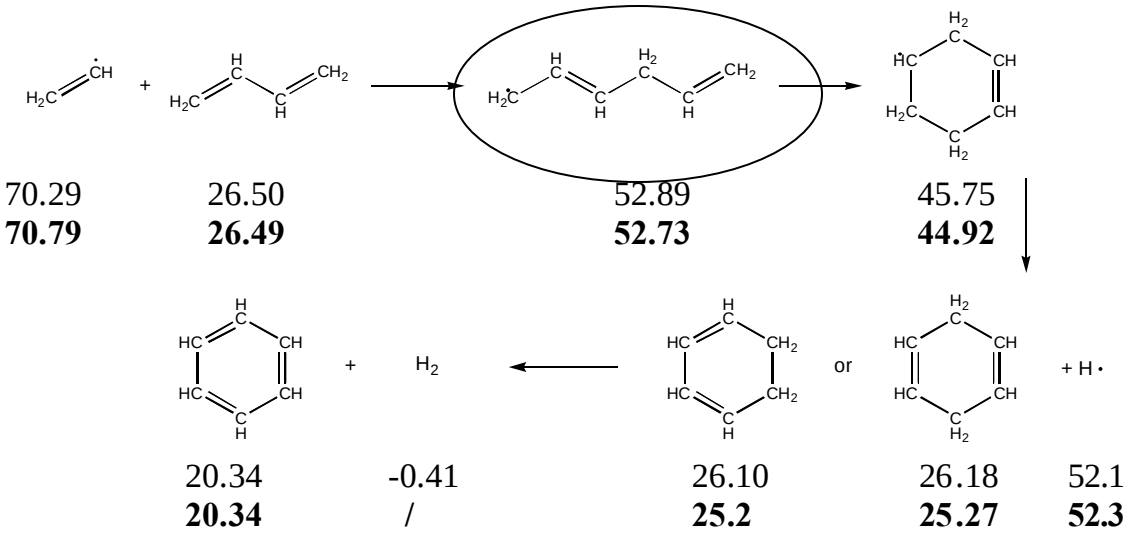

70.29	26.50	52.89	45.75	20.34	-0.41	26.10	26.18	52.1
70.79	**26.49**	**52.73**	**44.92**	**20.34**	/	**25.2**	**25.27**	**52.3**

C_4+C_2 mechanisms

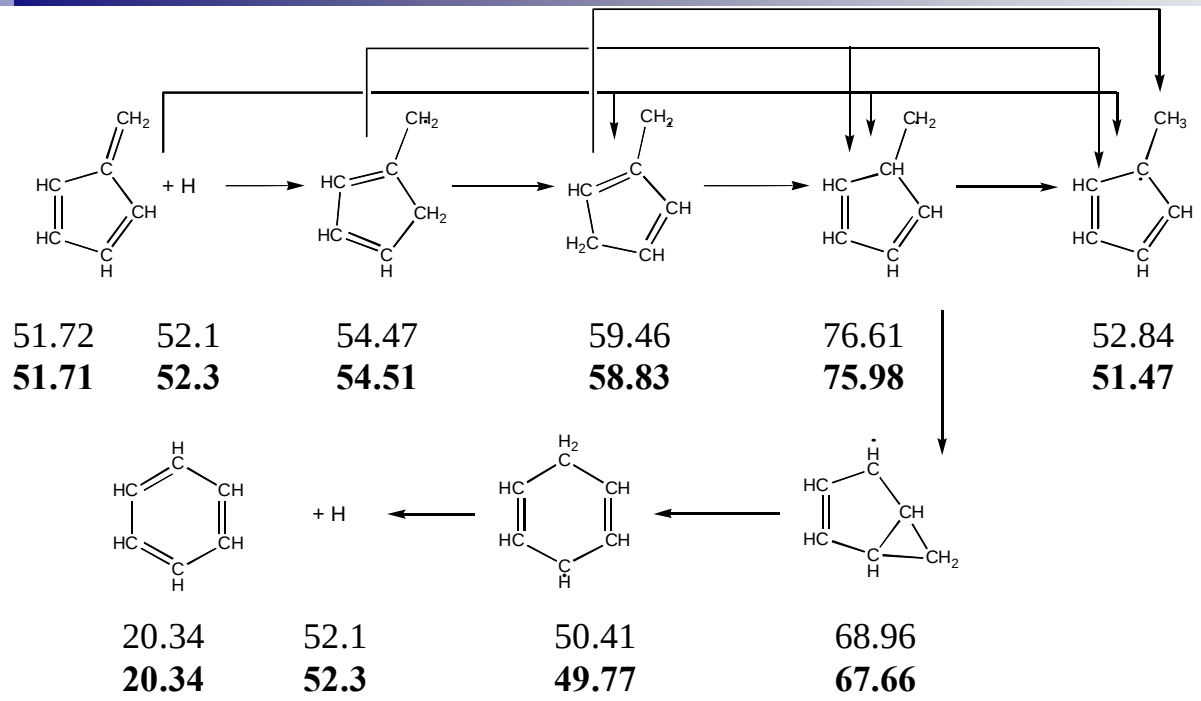

Fulvene isomerisation to benzene

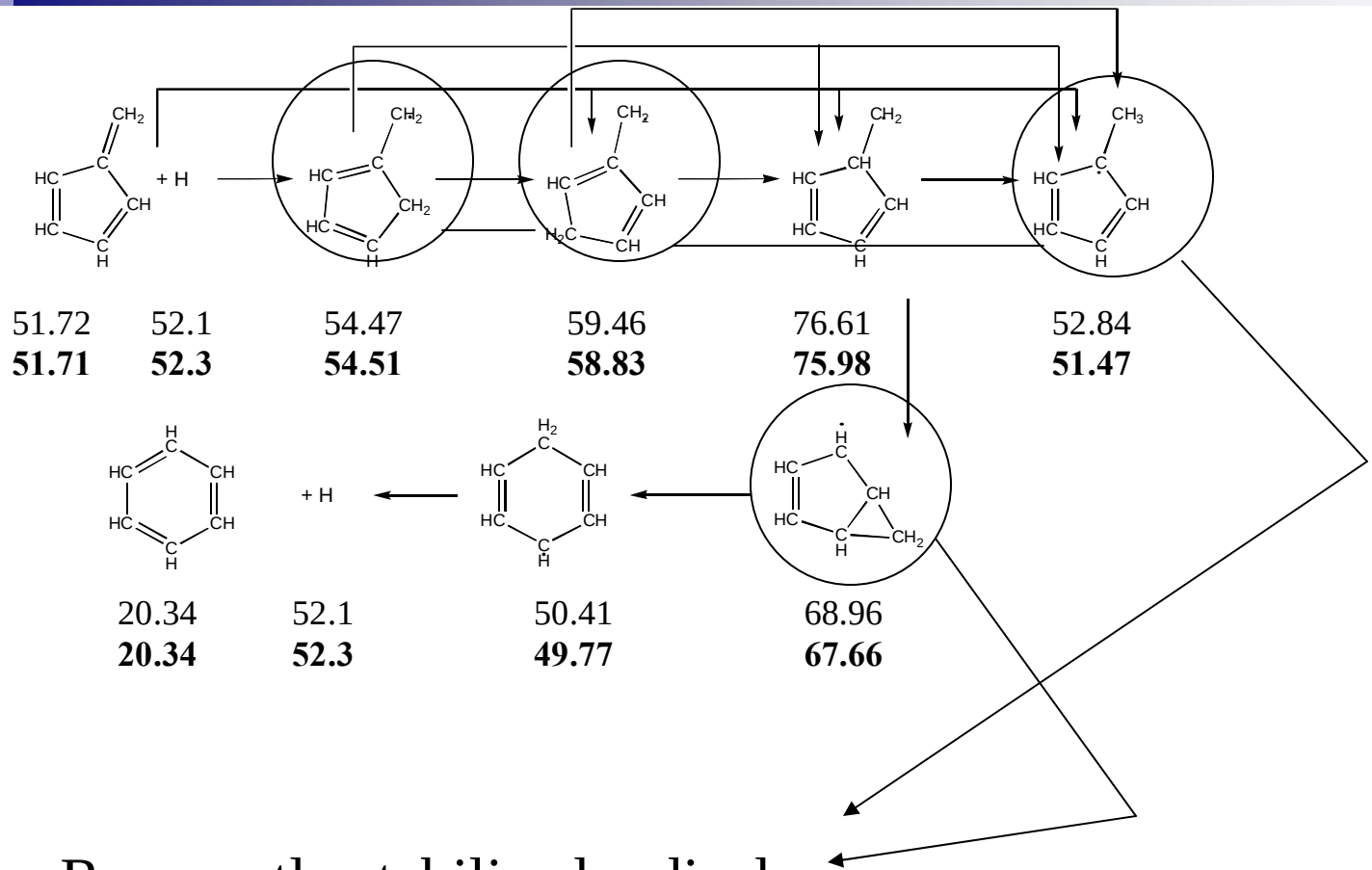

Resonantly stabilized radicals

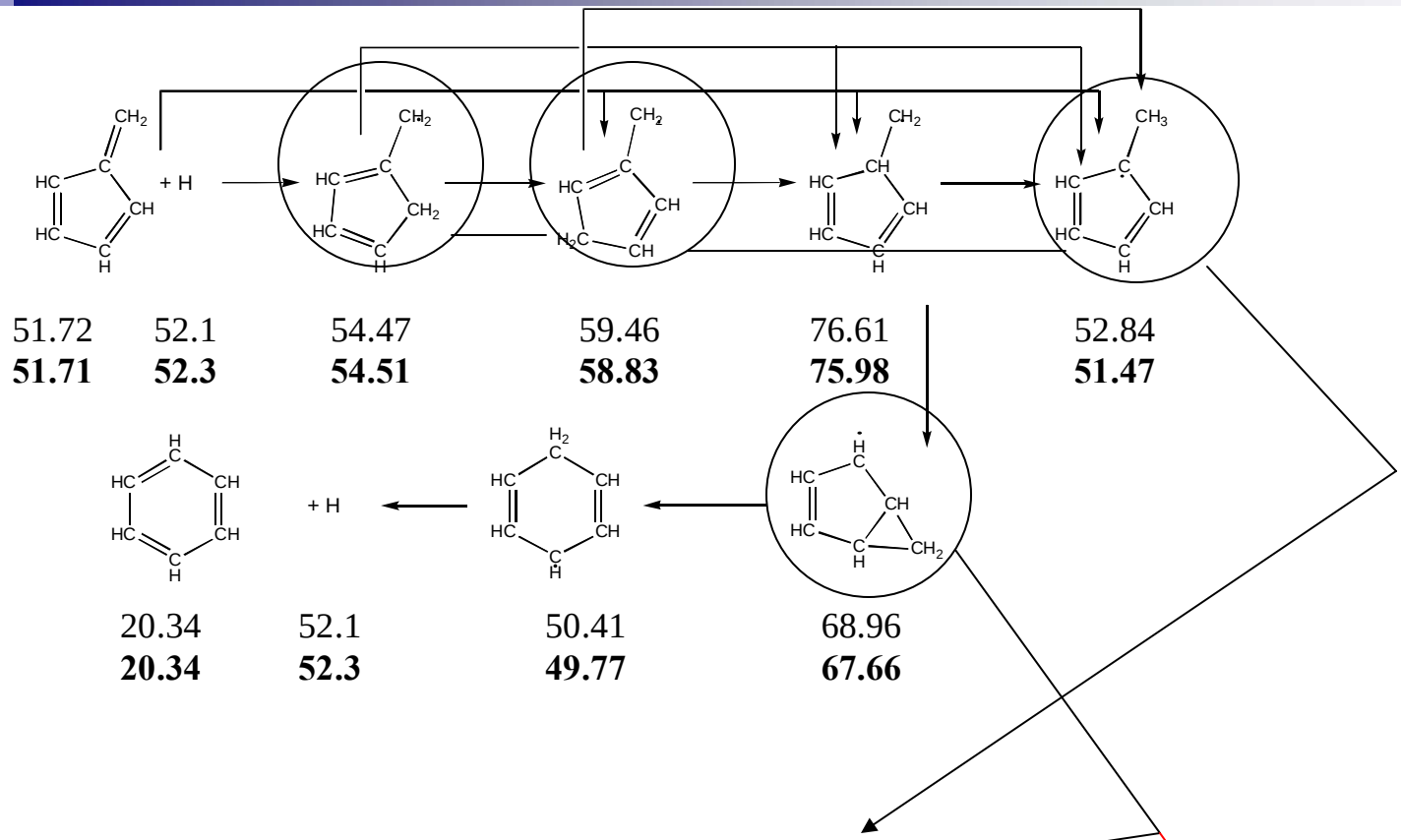

Resonantly stabilized radicals

Strained compound

Conclusions

- M1 and M3 methods do well for unstrained hydrocarbons
- Error of 1-2 kcal.mol^{-1} on strained hydrocarbons
- Spin contamination issues on resonantly stabilized radicals

Good ring formation modelling needs

- **Good understanding of the mechanisms**
- Accurate thermodynamic data
- **Reliable rate constants**

Rate constants and mechanisms

WORK IN PROGRESS

Rate constant of elementary reactions

- Transition states between reactants and products
- Better understanding of the mechanisms

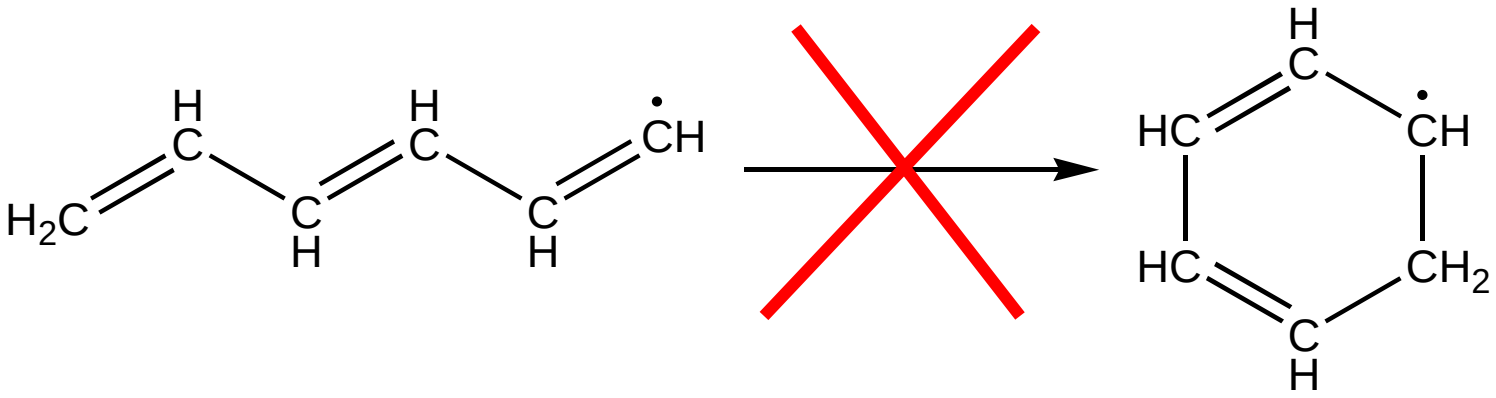

WORK IN PROGRESS

TST rate constant

$$k = \kappa \frac{k_B T}{h} \left(\frac{RT}{p}\right)^{-\Delta n} e^{\left(\frac{\Delta S^{\neq}}{R}\right)} e^{\left(\frac{-\Delta H^{\neq}}{RT}\right)}$$

$$A = \kappa e^{1-\Delta n} \frac{k_B T}{h} \left(\frac{RT}{p}\right)^{-\Delta n} e^{\left(\frac{\Delta S^{\neq}}{R}\right)}$$

$$E_a = \Delta H^{\neq} - (\Delta n - 1)RT$$

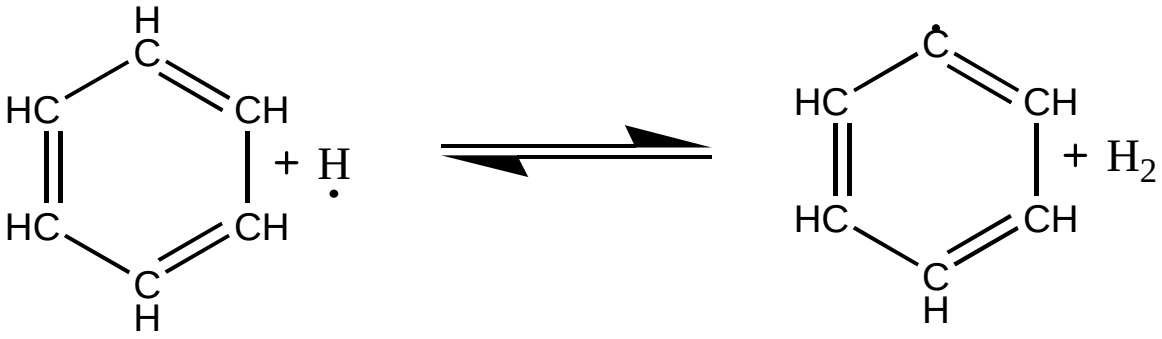

- Hydrogen abstraction from benzene
- Compared with available results

WORK IN PROGRESS

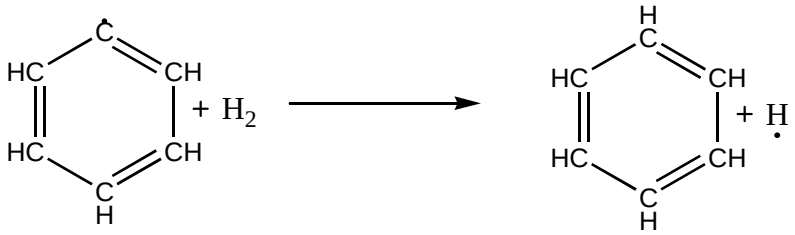
HC
CH
HC
CH
C
H
+ H2
H
C
HC
CH
HC
CH
C
H
+ H

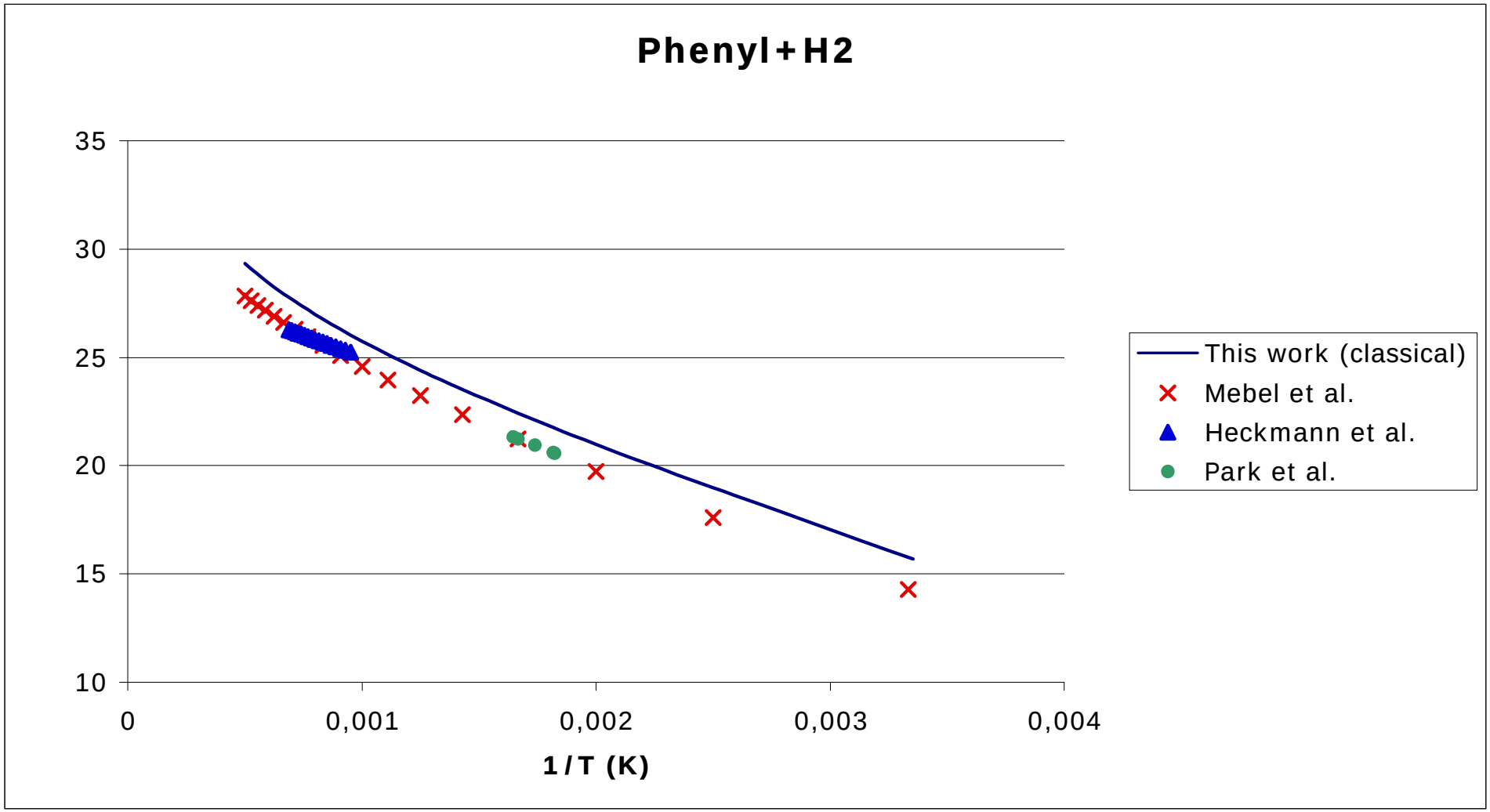
Phenyl+H2
35
30
25
20
15
10
0
0,001
0,002
0,003
0,004
1/T (K)
This work (classical)
Mebel et al.
Heckmann et al.
Park et al.

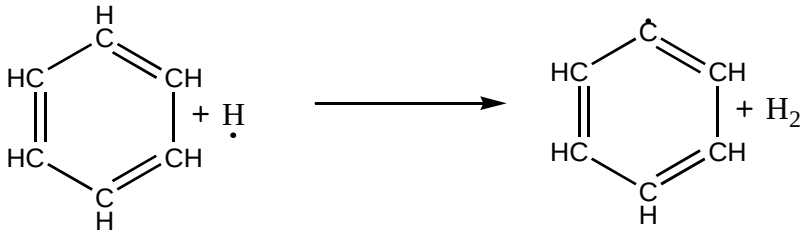
H
C
HC
CH
+ H
HC
CH
C
H
C
HC
CH
+ H2
HC
CH
C
H

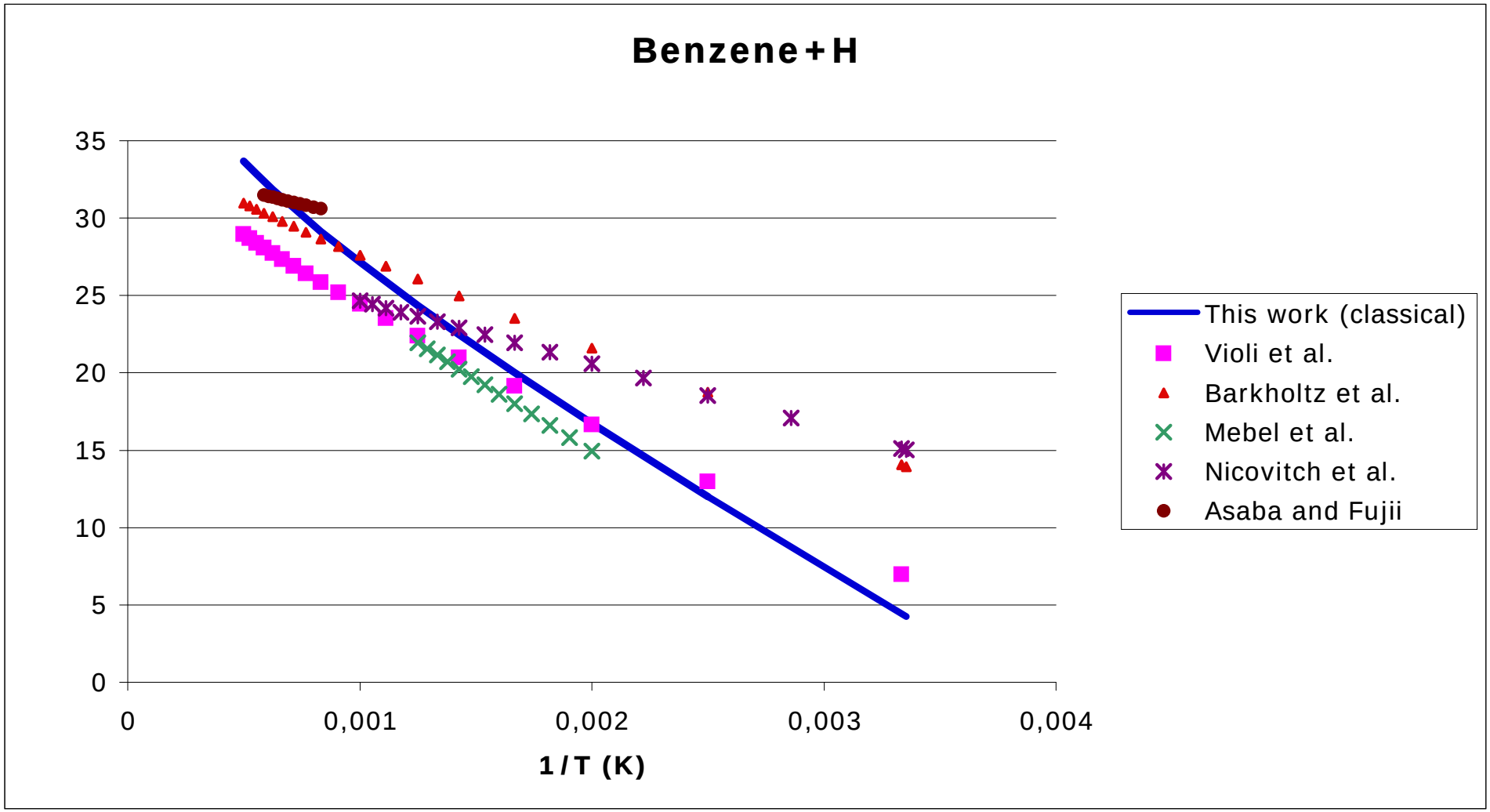
Benzene+H
35
30
25
20
15
10
5
0
0
0,001
0,002
0,003
0,004
1/T (K)
This work (classical)
Violi et al.
Barkholtz et al.
Mebel et al.
Nicovitch et al.
Asaba and Fujii

Perspectives

- Application of TST to complete mechanisms
- Tunnelling effects
- Pressure effects

Acknowledgement

Thanks to :
The Wallonia region
The FNRS
All members of Combustion and Quantum Chemisty laboratories at UCL

Subtask 2.4F

Theoretical Determination of Thermodynamic Data of Precursors of the First Aromatic Ring in Flames

Xavier LORIES, Jacques VANDOOREN† and Daniel PEETERS**

*Laboratoire de Chimie Quantique, †Laboratoire de Chimie de la Combustion,

Université Catholique de Louvain, Bâtiment Lavoisier, place Louis Pasteur 1,

B-1348 Louvain-la-Neuve, Belgium.

Abstract: The combustion of hydrocarbons in rich mixtures leads to the formation of polycyclic aromatic hydrocarbons (PAH). The formation of the first aromatic ring from light molecules is the rate-limiting step of the formation of PAH. But to correctly model the formation of that first ring, thermodynamic data of the involved species must be known precisely. Most of the compounds appearing in suggested mechanisms for benzene formation are radicals for which very often experimental data are not available. In this work, the G3B3 method has been used to determine the heats of formation of compounds involved in benzene formation mechanisms in hydrocarbon flames.

Introduction

Nowadays, the combustion of hydrocarbons is vastly used in transportation, heating, and power generation. Most of those burning systems are responsible for the formation of airborne species such as polycyclic aromatic hydrocarbons (PAH), which are important pollutants[1] and carcinogens[2]. The good understanding of the mechanisms leading to their formation is therefore very important from environmental and healthcare points of view. The search of such mechanisms has already motivated a lot of researches[3,4,5,6,7,8].

It is considered that the rate-limiting step in the pathways leading to PAH is the formation of the first aromatic ring[9]. A number of mechanisms have been suggested and used in different attempts to describe the formation of that first ring. All the proposed mechanisms involve radical species, for which thermodynamic properties have been determined with low accuracy or are not known. This lack of information leads to modelling failures.

The aim of this work is to determine, by quantum chemistry methods, the missing thermodynamic data needed to complete the models and hopefully improve their quality.

In order to make a first step toward better modelling, heats of formation of different reactants, products and intermediates involved in benzene formation are calculated.

Model Chemistry methods

Nowadays, the best methods to obtain thermodynamic data from a computational point of view are the Wn (n=1,2,3…) methods of J. L. Martin[10,11] , the Gn (n= 1, 2, 3, …) methods of Pople and co-workers[12,13] and the CBS methods developed by Peterson[14,15]. Those methods all imply a combination of different energies computed at different levels of theory. They aim at attaining energy with experimental accuracy and should provide “best energies” allowing computing reliable heats of formation. The method we have chosen is G3B3[16], which differs from G3 by the use of B3LYP geometries and frequencies.

Energies for species appearing in figures II to VII were calculated using that procedure. This method implies an optimized B3LYP/6-31G(d) geometry and frequencies calculation computed at the same level. These calculations are followed by single point calculations at full fourth order Møller-Plesset (MP4SDTQ hereafter simply noted MP4) level using 6-31G(d), 6-31+G(d) and 6-31G(2df,p) basis sets. Another single point calculation is computed using Quadratic Configuration Interaction with all Single and Double excitations and connected non-iterative Triple excitations (hereafter noted QCISD(T)) with a 6-31G(d) basis set. Finally a second order Møller-Plesset (MP2) calculation using the G3 Large basis is carried out. Those single point calculations allow obtaining corrections that can be added a posteriori to the B3LYP energy. The final G3B3 energy is obtained by an additive scheme using equations (1) to (5)

$$E(G3B3) = E\left[MP4(FC)/6-31G(d)\right] + \Delta(+) + \Delta(2df,p) + \Delta(QCI) + \Delta(G3L) + \Delta(SO) + \Delta(HLC) + \Delta(ZPE) \quad (1)$$

Where the first correction, given by equation (2) is used to take into account the effects of the diffuse functions. The next one (equation (3)) is used to consider the effect of polarization functions.

$$\Delta(+) = E\left[MP4(FC)/6-31+G(d)\right] - E\left[MP4(FC)/6-31G(d)\right] \quad (2)$$

$$\Delta(2df,p) = E\left[MP4(FC)/6-31G(2df,p)\right] - E\left[MP4(FC)/6-31G(d)\right] \quad (3)$$

Effects of configuration interaction are introduced by Δ(QCI) (equation (4)).

$$\Delta(QCI) = E\left[QCISD(T)/6-31G(d)\right] - E\left[MP4(FC)/6-31G(d)\right] \quad (4)$$

Using the G3Large basis set includes the remaining effects, such as core correlation.

$$\Delta(G3L) = E\left[MP2(FU)/G3\text{Large}\right] - E\left[MP2(FC)/6-31G(2df,p)\right] - \left(E\left[MP2(FC)/6-31+G(p)\right] - E\left[MP2(FC)/6-31G(p)\right]\right) \quad (5)$$

In those equations, *FU* indicates that the inner shells are included into the excitation space, while they are excluded by the frozen core approximation (*FC*).

$\Delta(SO)$ is a spin orbit correction used only in atomic calculations, and $\Delta(HLC)$ is a two-parameter empiric correction depending on the number of alpha and beta electrons. This final correction is supposed to bring us close to the exact energy. All calculations were performed using the Gaussian 03 package[17].

Computation of Heats of formation

The objective of this work is to obtain precise thermodynamic data for those hydrocarbons appearing in the various mechanisms of benzene formation (Fig. II-VII) and for which no experimental data are available.

One could imagine that using the "best" energies deduced from a model chemistry scheme, reactions energies, namely enthalpies of formation, could be obtained within experimental precision. Nevertheless, such assertion must be confirmed. To this end, three different methods may bring the required information to calculate the heats of formation at 298.15 K. The use of different calculation methods has thus different purposes. The first one is to determine the best method to deduce heats of formation. This led us to add a hydrocarbon test set (included in Table I) to the data. The second comes from the fact that, for most compounds of interest, no experimental values are available. The comparison between results from different methods allows checking their quality by discussing the similarity (or dissimilarity) of obtained values.

One method (M1) uses the atomization scheme[18,19]. According to this scheme, the heat of formation for a C_nH_m hydrocarbon is obtained by equations (6) to (8).

$$\Delta H_f^o(C_nH_m,0K) = n\Delta H_f^o(C,0K) + m\Delta H_f^o(H,0K) - \sum D_0 \quad (6)$$

Where ΣD_0 are the calculated atomization energies:

$$\sum D_0 = n\varepsilon_0(C,0K) + m\varepsilon_0(H,0K) - \varepsilon_0(C_nH_m,0K) \quad (7)$$

ε_0 *(X, 0K)* being the energy of X at 0K

Atomic heats of formation are taken from literature[20] and are for carbon and hydrogen 169.98 and 51.63 kcal.mol^{-1} respectively. The next step corrects the value at 0K to obtain the heat of formation at 298.15 K (equation (8)). Values for atomic enthalpy corrections are 1.01 kcal.mol^{-1} for hydrogen and 0,25 kcal.mol^{-1} for carbon.

$$\Delta H_f^o(C_nH_m,298K) = \Delta H_f^o(C_nH_m,0K) + \left[H(C_nH_m,298K) - H(C_nH_m,0K)\right] - n\left[H(C,298K) - H(C,0K)\right] - m\left[H(H,298K) - H(H,0K)\right] \quad (8)$$

Also heats of formation can be calculated from heats of reaction through different procedures. The first one involves complete hydrogenation reactions (M2). The second one (M3) uses the isodesmic concept[21]. An isodesmic reaction retains the number and nature of bonds on both sides of the reaction. Examples are shown on figure I. These latter processes have the advantage of aiming to conserve the errors and therefore cancel them out of the computation of heats of reaction.

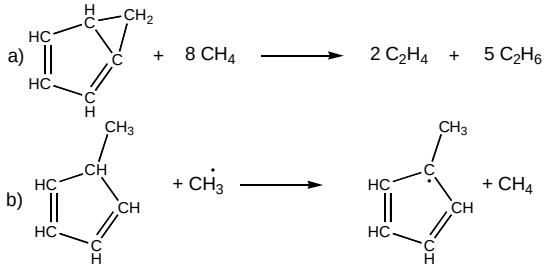

Figure I : Exemple of isodesmic reactions : a) for a molecule , b) for a radical

For commodity, the three methods presented will from now on be referred to as, respectively, M1, M2 and M3.

The reference molecules used were methane, ethane, ethylene and acetylene for molecular species and the methyl radical for radical species. Their recommended heats of formation are –17.89, -20.04, 12.54, 54.19, and 34,82 kcal.mol^{-1} respectively.

As isodesmic processes refer to well-defined references, which must retain the structural information between reactants and products, various choices of reactants can be considered. More precisely, when microcycles such as cyclopropane or cyclobutane are part of the structural pattern, it is worthwhile to introduce these molecules as references reactants and introduce them explicitly as a member of the set. These reactions will be referred to as M3-2 (cyclopropane) and M3-3 (cyclobutane).

The Mean Deviation (MD) allows comparison of the results with experimental data, which in the best case, should come out close to zero. The Mean Absolute Deviation (MAD equation (9)) brings another pertinent information as well as the minimum and maximum absolute deviation (MIN and MAX) of the set.

$$MAD = \frac{1}{n}\sum_{i=1}^{n}\left|\exp_i - calc_i\right| \quad (9)$$

Where n is the number of observations, exp_i and $calc_i$ are respectively the experimental and calculated heat of formation for the *ith* species.

Results and discussion

Heats of formation were obtained with the three different methods for a set of reference hydrocarbons, in order to evaluate the precision of each method.
Table I gives the results for the reference hydrocarbons using the three methods.
Both M1 and M3 show much better precison (smaller MAD), both having MAD values under 1 kcal.mol^{-1}. In terms of maximal deviations, M3 is the only method having a maximum deviation under 2 kcal.mol^{-1}. All three methods have near-zero minimum absolute deviation

Table I : Heats of formation for the reference molecules using the three different methods . (kcal.mol^{-1})

	Expnt[a]	M1	M2	M3
allene	45.53	44.96	43.56	45.26
propyne	44.32	44.09	42.69	44.14
cyclopropene	66.23	68.24	66.84	68.13
propene	4.879	6.10	5.12	6.19
cyclopropane	12.7	13.45	12.46	13.12
propane	-25.02	-24.96	-25.53	-25.09
1-butene-3-yne	70.04	68.82	66.67	68.97
1,3-butadiene	26	26.50	24.77	26.69
1,2-butadiène	38.7	39.56	37.83	39.75
methylene-cyclopropane	48	46.26	44.53	46.04
bicyclobutane	51.9	54.32	52.59	53.69
cyclobutene	37.5	39.31	37.58	39.09
1-butyne	39.48	39.69	37.96	39.63
2-butyne	34.68	34.55	32.82	34.49
cyclobutane	6.8	7.08	5.77	6.65
2-butene (E)	-2.58	-2.48	-3.80	-2.51
2-butene (Z)	-1.83	-1.02	-2.34	-1.05
isobutene	-4.29	-2.36	-3.68	-2.39
butane	-30.03	-29.95	-30.85	-30.19
isobutane	-32.07	-31.90	-32.80	-32.14
cyclopentadiene	33.2	32.60	30.13	32.49
spiropentane	44.23	44.56	42.50	43.82
cyclopentane	-18.26	-17.57	-19.22	-18.12
2-pentene (Z)	-6.7	-5.76	-7.41	-5.90
pentane	-35.08	-34.95	-36.18	-35.30
benzene	19.82	20.34	17.13	20.34
bismethylene-cyclobutene	80.04	81.23	78.01	81.22
1,3-cyclohexadiene	25	26.10	23.30	25.88
1,4-cyclohexadiene	25.04	26.18	23.38	25.96
1,3,5-hexatriene (E)	40	39.78	36.98	39.97
135 hextriene (Z)	41	41.36	38.56	41.55
toluene	11.95	11.87	8.33	11.76
	MD	-0.47	1.35	-0.34
	MAD	0.75	1.49	0.69
	MAX	2.42	3.62	1.96
	MIN	0.06	0.08	0.03

(a): Experimental values are taken from the National Institute of Standards ant Technology (NIST) Chemistry Web-book[22] .

One can conclude that the overall quality of the results is quite satisfactory and that some confidence may be given to the theoretically obtained results. Regarding Table I, isodesmic values present the smallest errors and should be recommended.
The use of the isodesmic reactions shows the best results, but for molecules containing three or four member rings important deviations appear. We used methods M3-2 and M3-3 in the hope of taking better account of the strain energy in those molecules. Results are shown in Table II.

Table II : Results for strained compounds using M3, M3-2 and M3-3 (kcal.mol^{-1})

	Expnt	M3	M3-2
cyclopropene	66.23	68.13	67.71
methylene-cyclopropane	48	46.04	45.61
bicyclobutane	51.9	53.69	52.84
spiropentane	44.23	43.82	42.97
			M3-3
Bismethylene-cyclobutene	80.04	81.22	81.37
cyclobutene	37.5	39.09	39.25

Method M3-2 improves only two out of the four concerned molecules. In fact, this method systematically lowers the calculated heat of formation and thus only improves the overestimated results. Method M3-3 does not improve results either but seems to raise the calculated value.
The M1 and M3 methods were then applied to the species involved in several benzene formation mechanisms.
The two main pathways to benzene involve either the recombinaison of propargyl radicals or the recombinaison of a C_4 and a C_2 species.
In this work, we have considered three propargyl recombinaison mechanisms. Those are the mechanisms of Miller and Melius[23] (Figure I), Miller and Klippenstein[24] (Figure II), and Alkemade[25] (Figure III). In figures II to VII, normal characters indicate M1 results in kcal.mol^{-1} and bold characters indicate M3 ones.

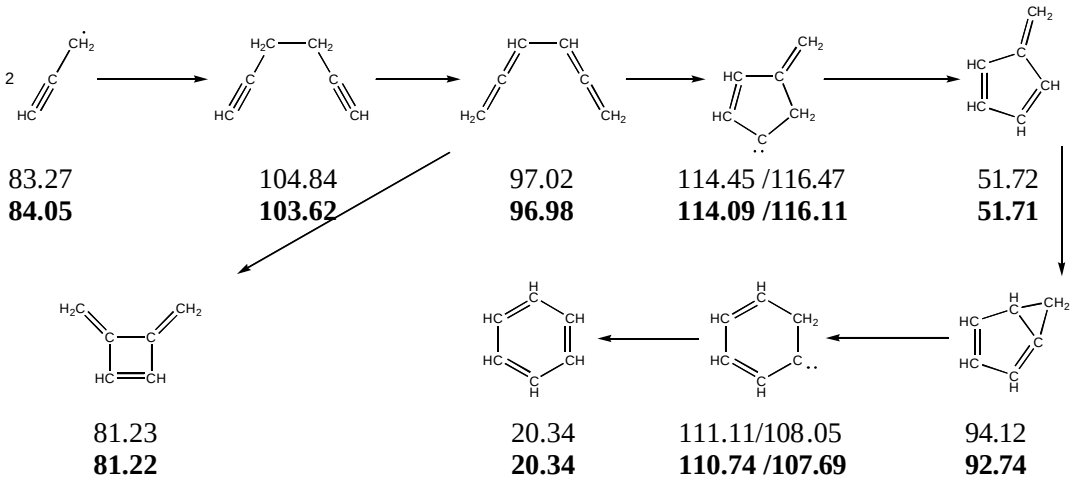

Figure II : Benzene formation mechanism through the recombination of propargyl radicals (Miller and Melius 1992)

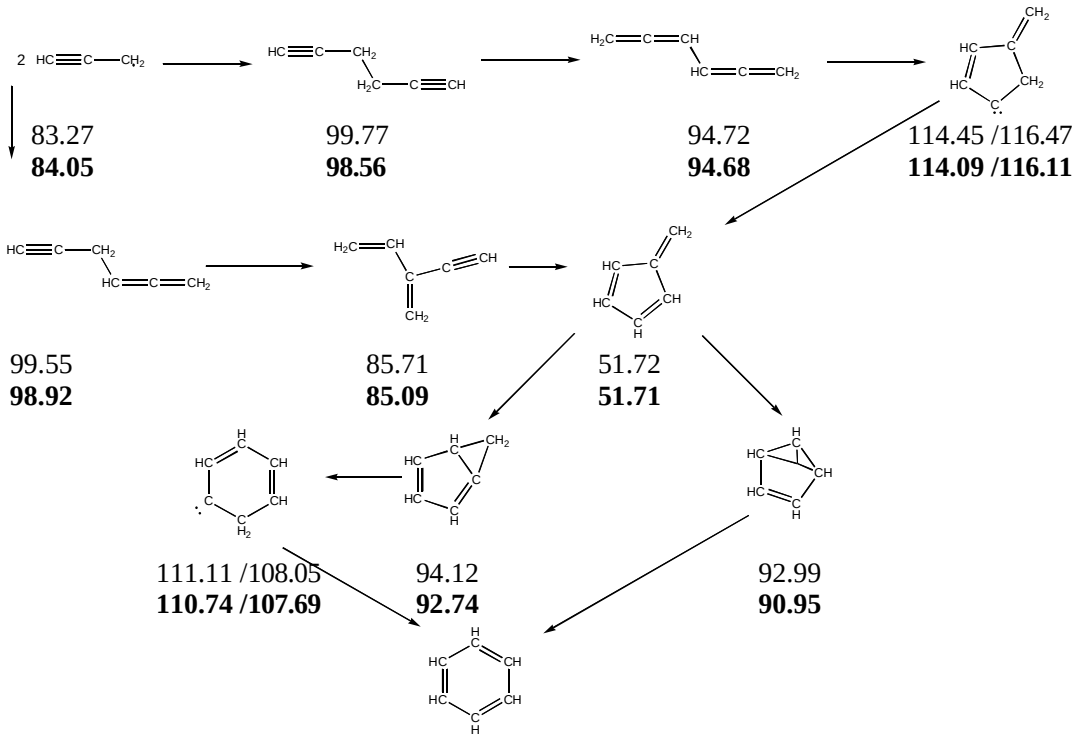

Figure III : Benzene formation mechanism through the recombination of propargyl radicals (Miler and Klippenstein 2003)

Heats of formation for biradical compounds are provided for the singlet (left) and the triplet (right) states.

Figures II and III show that fulvene is an important intermediate in benzene formation mechanisms from propargyl recombinaison. Experimental data is available for that compound and is 53.5 kcal.mol^{-1}. This value is about 2 kcal.mol^{-1} away from the calculated value. This deviation is higher than the usual deviation for unstrained molecules.

The experimental heat of formation is also available for the propargyl radical. Its value is 81 kcal.mol^{-1} which is much lower than the M1 and M3 calculated values. Since propargyl is a relatively small molecule, the calculated value may be compared with even more precise CBS-APNO results. Those calculations give a heat of formation of 82.24 kcal.mol^{-1}. That result is much closer to the experiment than the G3B3 one. We may therefore consider that the difference between the G3B3 results and the experimental results comes from remaining errors in the calculation method, such as for example spin contamination, which is known to be important in resonantly stabilized radicals..

We also have to mention that all the propargyl recombination mechanisms involve strained intermediates. As discussed above, errors on those compounds are expected to be a little higher than the others.

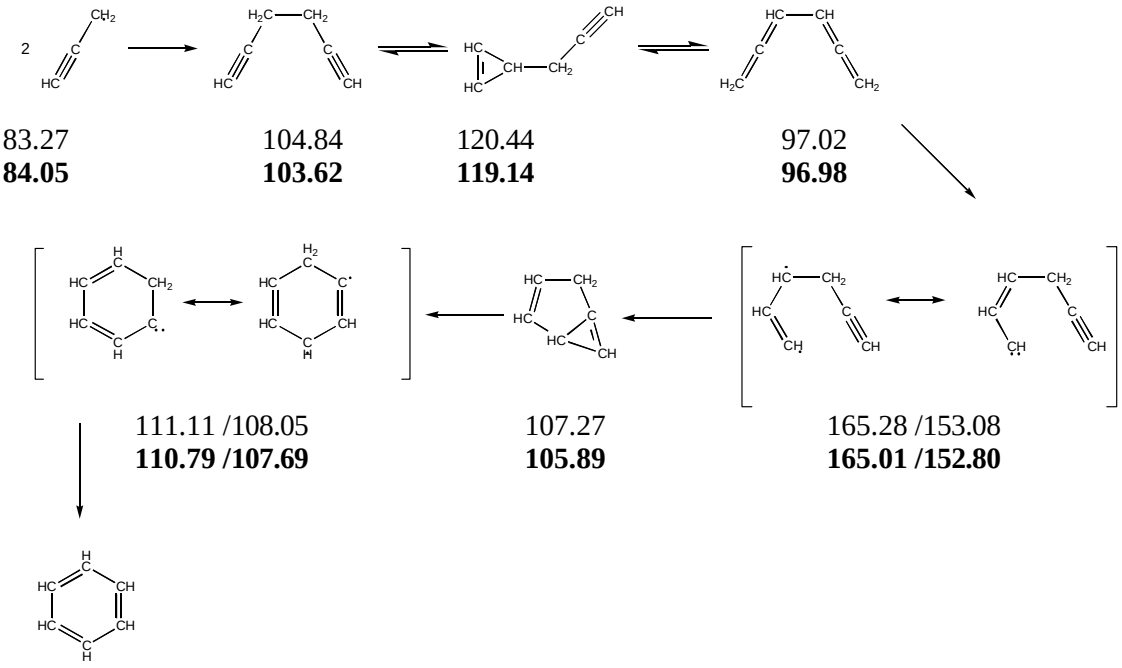

Figure IV : Benzene formation mechanism through the recombinaison of propargyl radicals (Alkemade 1989)

The mechanisms considered for the C_4+C_2 pathways are those of Cole et al[26] (Figure V and VI).

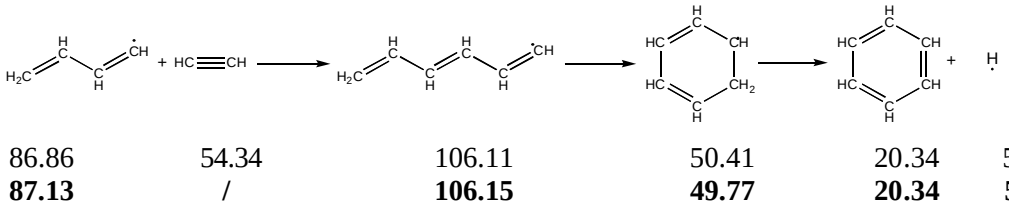

Figure V : Benzene formation mechanism through addition of acetylene on butadienyl radical. (Cole et al. 1984)

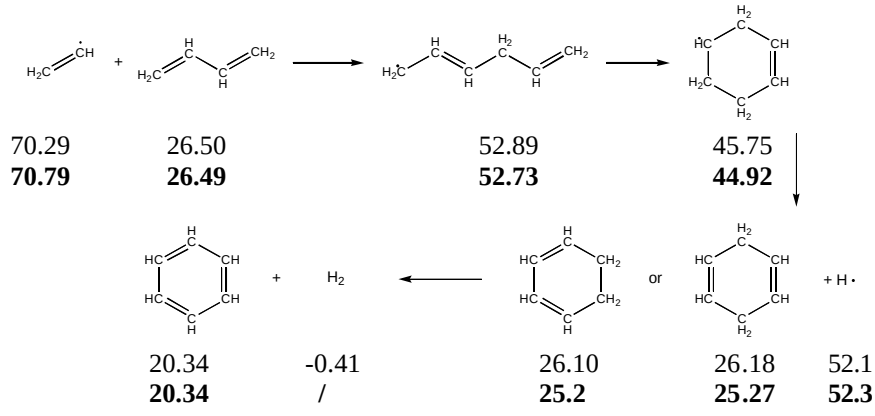

Figure VI : Benzene formation mechanism through addition of vinyl radical on butadiene. (Cole et al. 1984)

The M3 value for atomic hydrogen comes from the reaction between molecular hydrogen and the methyl radical.
Finally, we considered the mechanism of fulvene isomerisation to benzene proposed by Miller and Melius (Figure VII).

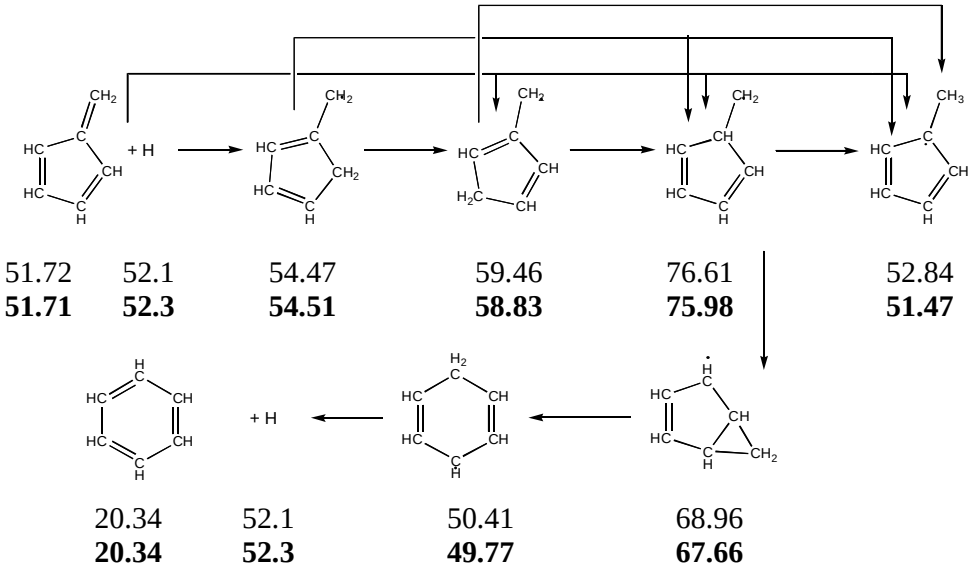

Figure VII : Isomerisation of fulvene to benzene (Miller and Melius 1992)

Differences between heats of formation of each monocyclic C_6H_7 radicals can be explained by their respective number of resonance forms. As propargyl, those latter compounds are resonantly stabilised radicals, therefore, we can expect a overestimation of their heats of formation due to spin contamination.

Conclusion

Heats of formation were determined for a set of hydrocarbons. Three methods were used, an atomization scheme, hydrogenation reactions and isodesmic reactions. When compared to experimental values for molecular species, they respectively showed –0.47, 1.35 and –0.34 kcal.mol^{-1} Mean Deviation and 0,75, 1.49, and 0.69 kcal.mol^{-1} Mean Absolute Deviation. Including the cyclopropane or the cyclobutane pattern into isodesmic scheme does not improve the results.
Afterwards, heats of formation for molecular, radical and biradical species, for which no experimental data is available, were calculated. Data were obtained using a G3B3 method combined to an isodesmic scheme. Even though no experimental comparison is available, this isodesmic scheme should provide data within 1 kcal.mol^{-1} and those heats of formation should be recommended for further use.
However, it is to be mentioned that this method still gives large differences with experimental values for two key compounds that are fulvene and propargyl.

ACKNOWLEDGMENT. The authors are indebted to the Belgian National Fund for Scientific Research (F.N.R.S.) for its financial support to this research and for its support to access computational facilities (FRFC project N°2.4556.99 and N°2.4502.05 on "Numerical Simulation"). X. Lories would like to thank Véronique Dias and Tom Leyssens for fruitful discussions.

References

[1] J. Toon, J. Sanders, Georgia Institue of Technology Research News, Georgia Tech Research News and Publication Office, Atlanta, September 27, 2002
[2] T. K. O. Nguyen, H. N. Le, L. P. Yin, Environmental Science and Technology, 36, 2002, p.833
[3] M. Frenklach, D. W. Clary, T. Yuan, W. C. Gardiner, Jr, S. E. Stein, Combustion Science and Technology, 50, 1986, p.79
[4] H. Richter, T. G. Benish, O. A. Mazyar, W. H. Green, J. B. Howard, Proceedings of the Combustion Institute, 28, 2000, p.2609
[5] N. M. Marinov, M. J. Castaldi, C. F. Melius, W. Tsang, Combustion Science and Technology,128, 1997, p.295
[6] M. Frenklach, D.W. Clary, W. C. Gardiner, S. E. Stein, Proceedings of the Combustion Institute , 20, 1984, p.887
[7] N. M. Marinov, M. J. Castaldi, C. F. Melius, W. Tsang, Combustion Science and Technology, 128, 1997, p.295
[8] M. Frenklach, D.W. Clary, W. C. Gardiner, S. E. Stein, Proceedings of the Combustion Institute, 21, 1986, p.1067
[9] H. Richter, J. B. Howard, Progress in Energy and Combustion Science, 26, 2000, p.565
[10] J. L. M. Martin, G. de Oliveira J. Chem. Phys., 111, 5, 1999, p.1843
[11] S. Parthiban, J. L. M. Martin, J. Chem. Phys., 114, 14, 2001, p.6014
[12] J. A. Pople, M. Head-Gordon, D. J. Fox, K. Raghavachari, L. A. Curtiss, J. Chem. Phys., 90, 10, 1989, p.5622
[13] L. A. Curtiss, K. Ragavachari, G. W. Trucks, J. A. Pople, J. Chem. Phys., 94, 11, 1991, p.7222
[14] G. A. Peterson, A. Bennett, T. G. Tensfeld, M. A. Laham, J. Mantzaris, J. Chem. Phys., 89, 4, 1988, p.2193
[15] J. W. Ochyerski, G.A. Peterson, J. Chem. Phys., 104, 7, 1996, p.2598
[16] A. G. Baboul, L.A. Curtiss, P. C. Redfern ; K. Raghavachari, J. Chem. Phys., 110, 16, 1999, p.7650
[17] Gaussian 03, Revision D.01,
M. J. Frisch, G. W. Trucks, H. B. Schlegel, G. E. Scuseria, M. A. Robb, J. R. Cheeseman, J. A. Montgomery, Jr., T. Vreven, K. N. Kudin, J. C. Burant, J. M. Millam, S. S. Iyengar, J. Tomasi, V. Barone, B. Mennucci, M. Cossi, G. Scalmani, N. Rega, G. A. Petersson, H. Nakatsuji, M. Hada, M. Ehara, K. Toyota, R. Fukuda, J. Hasegawa, M. Ishida, T. Nakajima, Y. Honda, O. Kitao, H. Nakai, M. Klene, X. Li, J. E. Knox, H. P. Hratchian, J. B. Cross, V. Bakken, C. Adamo, J. Jaramillo, R. Gomperts, R. E. Stratmann, O. Yazyev, A. J. Austin, R. Cammi, C. Pomelli, J. W. Ochterski, P. Y. Ayala, K. Morokuma, G. A. Voth, P. Salvador, J. J. Dannenberg, V. G. Zakrzewski, S. Dapprich, A. D. Daniels, M. C. Strain, O. Farkas, D. K. Malick, A. D. Rabuck, K. Raghavachari, J. B. Foresman, J. V. Ortiz, Q. Cui, A. G. Baboul, S. Clifford, J. Cioslowski, B. B. Stefanov, G. Liu, A. Liashenko, P. Piskorz, I. Komaromi, R. L. Martin, D. J. Fox, T. Keith, M. A. Al-Laham, C. Y. Peng, A. Nanayakkara, M. Challacombe, P. M. W. Gill, B. Johnson, W. Chen, M. W. Wong, C. Gonzalez, and J. A. Pople, Gaussian, Inc., Wallingford CT, 2004.
[18] R. J. Berry, D. R. F. Burgess, M. R. Nyden, M. R. Zacharia, M. Schwartz, Journal of Physical Chemistry, 99,1995, p.17145
[19] L. A. Curtiss, K. Ragavachari, P. W. Deutsch, J. A. Pople, J. Chem. Phys., 95, 4, 1991, p.2433
[20] L. A. Curtiss, K. Raghavachari, P. C. Redfern, J. A. Pople, J. Chem. Phys., 106, 1997, p.1063

[21] W. J. Hehre, R. Ditchfield, L. Radom, J. A. Pople, Journal of the American Chemical Society, 92, 16, 1970, p. 4798

[22] H.Y. Afeefy, J.F. Liebman, and S.E. Stein, "Neutral Thermochemical Data" NIST Chemistry WebBook, NIST Standard Reference Database Number 69, Edited by. P.J. Linstrom and W.G. Mallard, June 2005, National Institute of Standards and Technology, Gaithersburg MD, 20899 (http://webbook.nist.gov).

[23] J. A. Miller , C. F. Melius, Combustion and Flame, 1992, 91 , p.21

[24] J. A. Miller, S. J. Klippenstein, J. Phys. Chem. A, 107, 2003, p.7783

[25] U. Alkemade, K. H. Homann, Zeitschrift für Physikalische Chemie, (Neue Folge), 161, 1989, p.1934

[26] J. A. Cole, J. D. Bittner, J. P. Longwell, J. B. Howard, Combustion and Flame, 56, 1984, p.51